WPI

Dual-Axis Solar Tracker:
Functional Model Realization
and Full-Scale Simulations

FRENCH DEVELOPMENT ENTERPRISES
energy solutions

Picture of a Simulation

Picture of a Simulation

Authors

Dante Johnson-Hoyte
Melanie Li Sing How
Myo Thaw
Dante Rossi

Keywords

Solar Tracker
Dual-Axis

Dual-Axis Solar Tracker:
Functional Model Realization and Full-Scale Simulations

A Major Qualifying Project Report

submitted to the Faculty of

WORCESTER POLYTECHNIC INSTITUTE

in partial fulfillment of the requirements for the

Degree of Bachelor of Science

by

Dante Johnson-Hoyte
Melanie Li Sing How
Dante Rossi
Myo Thaw

Date:
March 10 2013

ABSTRACT

The use of a highly portable, efficient solar tracker can be very useful to applications of the military, industrial, or residential variety. To produce an efficient solar generation system, a scaled down dual-axis solar tracker was designed, built and tested. At most, the solar tracker was perpendicular to the light source within 3 degrees.

ACKNOWLEDGEMENTS

LIST OF FIGURES

	Author
Introduction	**Melanie**
Research background: part 1	**Johnson**
Research background: part 2	**Jennifer**
Research background: part 3	**Rossi**
Research background: part 4	**Myo**
Research background: part 5	**Melanie**
Goal statement	**???**
Design specifications	**Melanie, Myo**
Design Description	**Melanie**
Electrical system	**Rossi/Johnson**
Sensor Testing	**Myo**

LIST OF TABLES

No table of figures entries found.

TABLE OF CONTENTS

1. INTRODUCTION:

Solar power is the fastest growing means of renewable energy production with grid connected solar capacity increasing on average by 60 % annually from 2004 to 2009 according to the National Center for Policy Analysis [A]. Yet solar energy contributes to only … The current situation of the more mature segment of solar energy production, the Photovoltaic (PV) solar cell technology, is one in which energy production is improving from….(energy capacity value)!! Stanford University Professor Stefan Reichelstein, author of the new working paper "The Prospects for Cost-Competitive Solar PV Power," believe the future of PV solar technologies look promising considering favorable location and continued federal tax subsidies [A] as well as state renewable standard protocol [B]. According to him, with the continued trend in decreasing cost of PV panels and government subsidies, PV Solar energy might become cost competitive in the next 10 years (subsidy-free), for commercial installations while for Utility-scale installations it will take longer [A]. The August 2010 White House report on the other hand predicted that PV solar power will reach grid parity by 2015. Regardless of the diverging predicted time period for grid parity equivalence with current price, it is unequivocal that for solar photovoltaic energy production to become a reality it has to compete with other available sources of energy.

Subsequently, it is believed that Solar tracking will contribute significantly in increasing the efficiency of energy collection from the PV panels. Novel Dual-Axis solar systems allow for precise control of the elevation and azimuth angle of the panel relative to the sun. Tracking is reported to potentially double the energy output of a fixed PV Solar system. The French Development Enterprises (FDE) are currently developing a patented Dual-Axis Solar system that in addition to tracking the sun via sensitive sensors (add more attributes), it can be rapidly deployable and transportable with an automatic?? default position in extreme weather conditions. Among the benefits of this remotely articulated solar tracker include a maximum tilting angle of 80 degrees with the horizontal axis to remove accumulated snow and sensitivity speed of …from one extreme position to the other. During the three months of tracking the sun with their commercial Single-Axis solar system, they have been obtaining a positive power efficiency of…(estimate from website they gave us) which …(state good or bad estimate for future dual axis STS).

This report will therefore focus on the force and stress analysis of the Dual-Axis Solar system (STS 444) different configuration under the critical wind and snow conditions. The second part of the report will be based on modeling a table-top sized prototype for the FDE to demonstrate the tilting and sensing-responsive abilities of the prototype to potential clients.

2. BACKGROUND

There is a great and growing need for renewable energy, in particular green energy. In years to come we will want a source of energy that will leave future generations with a sustainable energy source. A few good reasons to improve our green energy market are because not only do we want to have renewable energy for future generations, but we also want to have a sustainable energy market in future. Green energy has shown sustainable growth in past years, where oil has obviously not. In order to power our homes, businesses, and most aspects of our daily lives we require electricity, which requires massive power plants and spending billions of dollars to run them. But what if we could avoid all the resources that are used generating this energy, and replace them with green energy that could provide power directly to the consumers like businesses, the military or even private homes.

The military will most likely be one the major user of renewable energy in the future. The department of defense plans on opening up 16 million acres of land for renewable energy development, which includes solar energy development. To highlight how new this is, the DOD only made this announcement in early August, meaning solar energy is a major market and a technology of great interest to our nation. There are also many other major solar energy projects that the military is partaking in such as The Sterling solar power renewable energy construction project which have supplied an Army depot outside Salt Lake City with approximately 30% of there power, potentially powering up to 400 homes. Another project is the renewable energy project at the U.S. Army Garrison Kaiserslautern in Kaiserslauter, Germany that will generate enough energy to power 500 homes. In future there are plans to generate enough power on military installations to power 750,000 homes by 2025.

Currently in order to run a military base large generators are required, which are reported to be not nearly as efficient as solar panels could be, and consume large amounts of fuel in order to run. The needs of future military installments are to have renewable energy sources that require less maintenance and are more energy efficient as opposed to petroleum. In addition, solar energy will not only be used for military bases, but also for mobile military units as well, which will be more efficient at providing soldiers energy for their equipment used in the field.

Overall it is dangerous to depend strictly on fossil fuels. It is dangerous politically, economically, and naturally. Politically we want the country to not have to depend on petroleum from other countries. Being dependent on other countries, especially as the top consumer of fossil fuels, would have a negative impact on our country in the future; that is when they resources disappeared. On the economic side, our country would be in better shape to be more self sustaining in future. On the environmental side, when it comes to burning these fossil fuels, although debated on how bad the environmental effect is, it is known to produce large amounts of carbon dioxide.

Some have complained about the true benefits of solar power, and argue that it is not cost effective enough to be worthwhile. On the other hand reports have shown that costs have gone down for something like installments at home, and that the payoff for installing them would be even greater. The cost per watt has been estimated at $4.85/Watt, which is said to be a 50% increase since 5 years earlier. Although the cost for at home installation is said to cost around $5,000, the life of solar panels is said to be incredibly long, and only lose around half a percent of their maximum power each year. This makes them a great technology to invest in and continue to develop, so that in future they can produce even more power. This way, states like California can reach their goal of 33% solar energy dependency by

2025. Like this many countries have started to make this move toward green energy and energy independence; this is because they know it is the energy of the future.

2.2. *what are the essentials of a solar panel in general and that of a solar tracker, list of component and function etc JENNIFER*

2.3. *Type of solar trackers (History/patents/publication) ROSSI*

The effectiveness of a solar tracker and PV technology in general, is directly correlated to the amount of sunlight that it is being exposed to; its power output is dependent on the amount of light that reaches the solar cell. PV technology is most efficient when it is greeted by a light source at a perfectly perpendicular angle, i.e. forming a 90 degree angle. In order to accomplish this in a real-world situation, the PV panel must move with the sun to maintain this perpendicular angle. [6] Mehleri, E.D., P.L. Zervas, H. Sarimveis, J.A. Palyvos, and N.C. Markatos. "Determination of the Optimal Tilt Angle and Orientation for Solar Photovoltaic Arrays." *Renewable Energy* 35.11 (2010): 2468-475.

This is where the necessity for solar tracking comes in. Solar tracking is not a new concept, though it is a considerably new concept compared to PV cells. Patents began to be filed in regards to solar tracking, and even before that regarding simple light sensing technology, soon after the commercial availability of efficient PV panels hit the market: about 50 years ago. [2http://www.google.com/patents/US4225781?printsec=abstract#v=onepage&q&f=false] Like most technology today, a large collection of solar tracking systems exist, ranging in price, effectiveness, reliability, etc. The design options for a solar tracking system must be taken into careful consideration to ensure that the system is maximizing its output from tracking the sun. If key aspects of the application needs were to be neglected, the solar tracker could actual under-perform a well-positioned stationary PV panel.

Even though solar tracking will inherently give a greater power output than a stationary PV panel, the option is not always ideal. Due to the increased cost for solar tracking technology versus stationary PV panels, solar tracking is not always the best option for a given application. If a stationary PV panel is utilized, it is strategically placed facing the sun. The considerations to be taken regarding PV panel placement is that the panel must be placed in a spot where it will always have a clear line of sight (LOS) to the sun, and the panel must be positioned at an optimal angle facing the equator, depending on its latitude on earth, see figure 1. [5] Stationary PV panels are a cheaper energy solution, but do not fully utilize the energy coming from the sun.
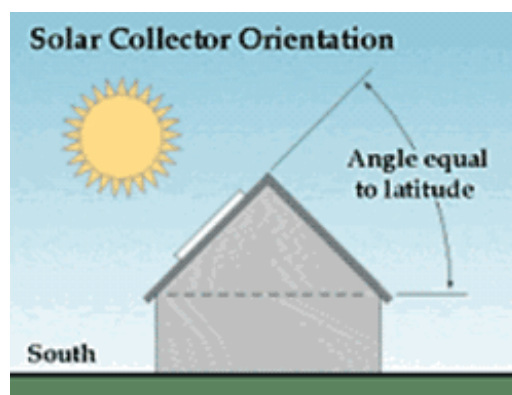

Figure 1: Stationary PV panel orientation

Due to the fact that the earth is rotating on a tilted axis and takes an elliptical path around the sun, a stationary PV panel's output will drastically vary throughout the year and even throughout the course of a day, see figure 2.
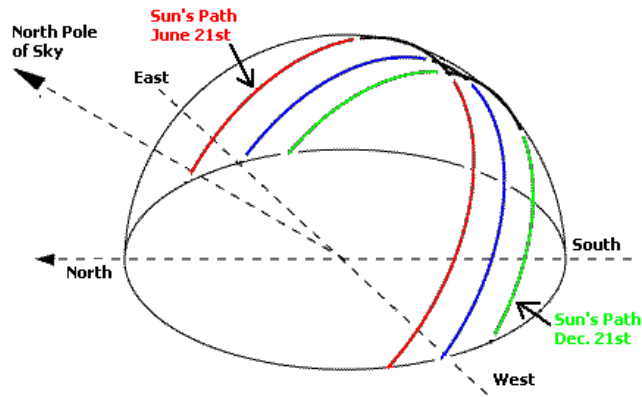

Figure 2: Earth's axis tilt/orbital path affecting Solar angle

Solar tracking obviously addresses these issues by actively following the sun in the sky. A standard PV panel will observe about 20-35% efficiency under ideal conditions, while solar tracking has been known to potentially double that with 50-60% efficiency under ideal conditions. [8] H. Mousazadeh et al., *A review of principle and suntracking methods for maximizing solar systems output*, Renewable and Sustainable Energy Reviews 13 (2009) 1800–1818. In general there are two main groups that can categorize solar trackers: single or dual axis trackers. Single axis trackers singularly follow the Sun's East-West (or even North-South) movement, while the two-axis trackers follow the Sun's exact movement, no mater what direction. Typically tracking is done, considering a single axis at a time, by using two photoresistors or PV cells used as sensors. These sensors are strategically placed next to one another and have a divider/tilted mount of some sort to create a voltage difference. This voltage difference is then used to determine which way the panel needs to turn to face the sun perpendicularly.

The first type of active solar collecting is single axis tracking. This is will result in a greater power output than stationary PV panels, but is also more costly to design and implement. Single axis solar trackers can either have a horizontal or a vertical axis. The horizontal type is used in regions near the equator where the sun gets very high at noon, thus not having to adjust to vertical changes so much as horizontal changes, see figure 3.

Figure 3: Horizontal single axis tracker

[7] The vertical type is used in high latitudes where the sun does not get very high, but summer days can be very long. Conversely, utilizing the fact that vertical movement does not have to be compensated for as much as horizontal movement, see figure 4.[7]

Figure 4: Vertical Single axis tracker

The second type of active solar collecting is dual axis tracking. This results in a much greater power output than a stationary PV panel, but is also the most costly and most complicated to design. Dual axis solar trackers have both a horizontal and a vertical axis and thus they can track the sun's apparent motion virtually anywhere in the sky no matter where it is positioned on earth, see figure 5. [5] P. Roth et al., *Cheap two axis sun following device*, Energy Conversion and Management 46 (2005) 1179–1192]

Figure 5: Standard Dual axis tracker

Many traditional solar PV applications employ dual axis trackers to position the solar panels perpendicular to the sun's rays. This maximizes the total power output by keeping the panels in direct sunlight for the maximum number of hours per day. [7]

[1] http://www.google.com/patents/US4031385?printsec=abstract#v=onepage&q&f=false

Inventors: Gene A. Zerlaut, Robert F. Heiskell
Original Assignee: Desert Sunshine Exposure Tests, Inc.
Current U.S. Classification: 250/203.4; 126/575; 126/578; 136/291; 356/139.01
International Classification: G01J 120

[2] http://www.google.com/patents/US4225781?printsec=abstract#v=onepage&q&f=false
Inventor: Burrell E. Hammons
Original Assignee: The United States of America as represented by the United States Department of Energy

Primary Examiner: Daniel O'Connor
Current U.S. Classification: 250/203.4; 126/573; 250/237.00R; 356/139.01

[3] http://www.google.com/patents?id=_FkuAAAAEBAJ&printsec=abstract&zoom=4#v=onepage&q&f=false
Inventor: Kei Mori
Primary Examiner: Ernest Austin, II
Current U.S. Classification: 250/208.2; 126/573; 356/121

[4] http://literature.rockwellautomation.com/idc/groups/literature/documents/wp/oem-wp009_-en-p.pdf
Solar Tracking Application (A Rockwell Automation White Paper)

[5]   P. Roth et al., *Cheap two axis sun following device*, Energy
Conversion and Management 46 (2005) 1179–1192

[6]   Mehleri, E.D., P.L. Zervas, H. Sarimveis, J.A. Palyvos, and N.C. Markatos. "Determination of the Optimal Tilt Angle and Orientation for Solar Photovoltaic Arrays." *Renewable Energy* 35.11 (2010): 2468-475.

[7]   Reda, Ibrahim, and Afshin Andreas. *Solar Position Algorithm for Solar Radiation Applications*. Tech. N.p.: National Renewable Energy Laboratory, n.d.

[8]   H. Mousazadeh et al., *A review of principle and suntracking methods for maximizing solar systems output*, Renewable and Sustainable Energy Reviews 13 (2009) 1800–1818.

2.4. *Specific improvement in mechanical design and ECE design over past generation solar trackers (from single to dual axis etc) MYO*

## Tracking system

Active tracking

Active tracking uses motors, gears, and actuators to position the solar tracker so that it is perpendicular to the sunlight. Trackers that use sensors to track the sun position inputs data into the controller, which in turns drives the motors and actuators to position the tracker. There are also trackers that uses solar map. Depending on the location, solar maps give information on where the sun is at different time of day throughout the year. Trackers that use solar map do not need sensors input to track the sun. But there are also tracker that uses both sensors and solar map. During sunny weather, the sensor would be used to track the sun. But during cloud-covered times, the information from the solar map would be used. It is important to track the sun even in cloudy condition since solar panels can produce energy during cloudy conditions.

Passive

Passive trackers use compressed gas to move the tracker. Depending on the position sunlight is falling on the gas containers difference in gas pressure is created, moving the tracker until it gets to an equilibrium position. The advantage of passive tracker is that the tracking system does not require a controller. But passive trackers are slow in response and are vulnerable to wind gusts.
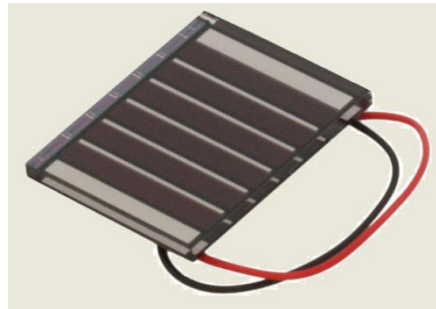
Sensors

Any device that is sensitive to the intensity of light can be used as solar tracking sensors. Two of those similar devices can be placed at an angle as shown in the figure below.
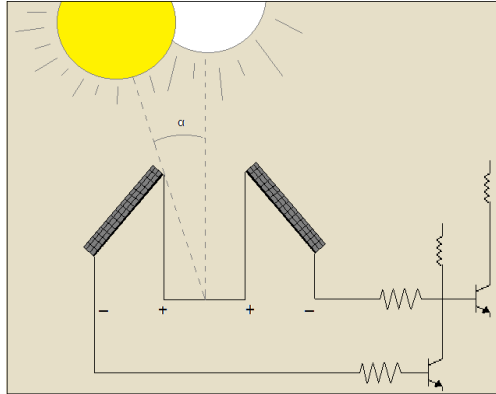
When the sun is on the left, the sensor on the left receives more light than the one on the left. If the sensors produce voltage with light intensity, the left sensor would produce more voltage than the one on the left. From the result, we can know that the sun is on the left. When the two sensors are outputting the same value, we know that the sun must be at the top, perpendicular to the sensor unit.

Photovoltaic cells

Photovoltaic cells, those when combined made up a solar panel, can be used to detect light intensity. It produces the maximum voltage when the sun is perpendicular to the cells. As the angle between the cell and the sunray decreases, the voltage also drops. When the cells are parallel with the sunlight, it will produce a minimum voltage.



Light Dependent Resistor (LDR)

Light dependent resistors or photoresistor is a type of resistor who resistance depends on the amount of light falling on the sensor. The resistor of LDR increases with decreasing light intensity.
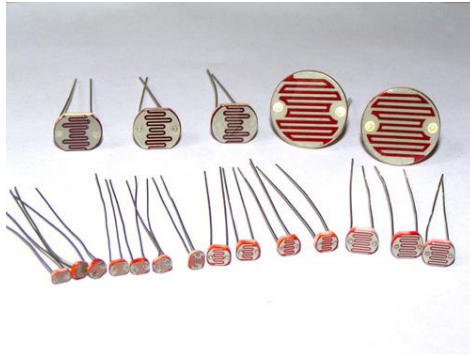
Different sizes of LDR being sold

Light Emitting Diode (LED)

Light emitting diode is a type of diode that products light when current flows through its terminal. But it also has a property of producing current when it receives light, just like a photodiode. As the light intensity increases, the current an LED produces also increases.
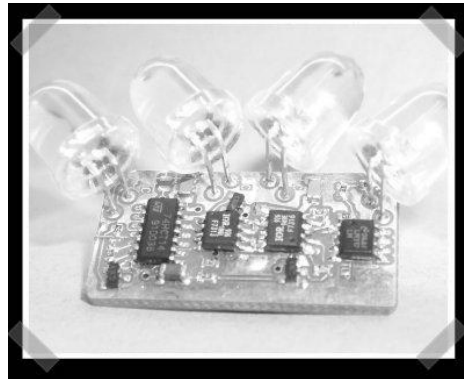
Photodiode

Controllers

The main purpose of the controller is to receive data from the sensors, process it, and give signals to drive the motors and actuators. Looking at it simply, a human can take the place of a controller. A person can see where the sun is and rotate the tracker manually to get the most energy. But it is not a feasible option for a long term or when there is more than one tracker, like in a solar power plant. So automated controllers become a necessity. Controllers must also take into account what to do when the sun sets, when the wind is too high, or other physical conditions.

Programmable Logic Controller (PLC)

PLC are like a mini computer, but its main purpose is to control processes that are repetitive. It has input terminal for analog and digital input, a processor to do arithmetic, and output terminal to control

machineries. It is mostly used in assembly lines. Since solar tracking is also a repetitive activity, a PLC can be programmed to take in data from the sensors, process the information, and output signals to the motors and actuators. Since PLC is an old technology, the devices are often bulky and also expensive.

ML 1500 PLC from Allen-Bradley

Microcontrollers

Microcontrollers can perform very similar tasks as PLCs, but the size of the device is much smaller. A processor, memory, and the input/output peripherals are all embedded into a single integrated circuit (IC) about the size of a fingernail. They are very cheap, costing around $3 for a single IC. But the disadvantage of microcontrollers is that they are made to control small appliances. Communication terminals such as LAN are not common in microcontroller boards, unlike the PLCs. So using microcontrollers for solar tracking in a power plant is not very feasible in terms of status monitoring and controlling them for maintenance. But it would be the best option for a home use tracker or for a prototype.
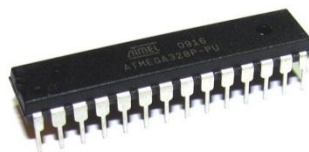
Atmel ATmega328 microcontroller (used in Arduino UNO boards)

Analog IC

Everything that a microcontroller can do can also be done by analog integrated circuits. There are analog ICs that are made just for the purpose of solar tracking. But when more features are wanted in the system, like tilting the solar panels to dispose the snow automatically, analog circuit design become inefficient, resulting in several ICs and devices on the controller board.

Mechanics

Slewing drive

The slewing drive makes sure of the worm drive mechanism to produce torque for rotating. It can be found in many types of machinery such as wind turbines, cranes, and telescopes. But they are also widely used in solar trackers to provide rotational movement, mainly in vertical direction. These are known as single axis slewing drive. Because slewing drive uses a worn drive system, it is self-locking or irreversible. This makes the slewing drive resistant to wind and other external forces on the trackers. A slewing drive is made by combining the gearing, bearings, seals, housing and other components into one single unit.

A single axis slewing drive made by Kinematics Manufacturing, Inc

**73 kg slewing drives begin assembled at Beijing Titanhorse Industry and Trading**

As demand for solar tracking increases, dual slewing drives are now in mass production. Two slewing drives and two motors are combined into one unit, which can be mounted on top of a tower. With the dual axis slewing drive, a single unit can provide both the horizontal and vertical rotations.

Custom designed dual axis tracking drive made by Conedrive

[http://www.conedrive.com/content/library/solar_appimg1.jpg]

Most of the dual slewing drive in production are intended for use in solar power plants, but smaller dual slewing drives are also available for home use, as the one shown below.
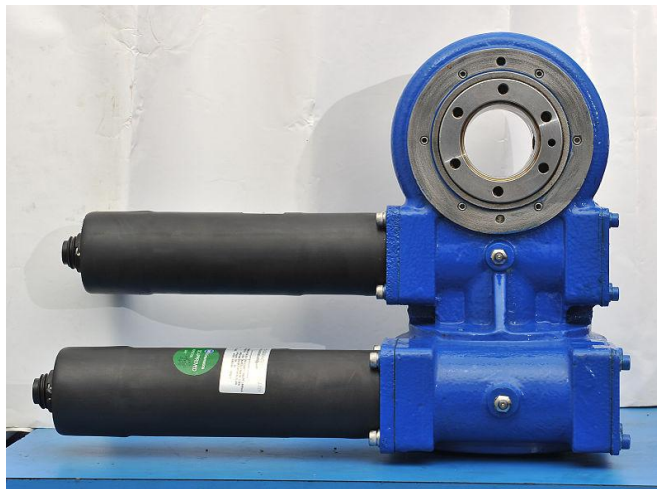
A dual axis slewing drive made by Kinematics Manufacturing, Inc

[http://en.wikipedia.org/wiki/File:Kinematics_Slewing_Drive.jpg]

There are also slewing drives that make use spur gear instead of the worm gear to achieve rotational motion. A motor connected to a small spur gear is mounted vertically, and as the motor rotates, the spur gear rotates itself against the teeth of a stationary ring gear. Both the internal and external ring gear can be used for this design. Because this type is not self-locking, the motor must have other locking mechanism to withstand external forces.

Spur gear driven slewing drive manufactured by IMO

Linear Actuator

A linear actuator creates motion in a straight line. There are many types of linear actuators available: mechanical, hydraulic, pneumatic, etc.   The most common is the mechanical linear actuator. Many of them use a screw and an electric motor to rotate the screw to produce a linear motion. Linear actuators that use acme screw are self-locking, compare to ball screw that is not. Some linear actuators have a variable resistor inside that changes in value depending on the location of the stroke. That resistor can be used to get feedback data on the location of the stroke.
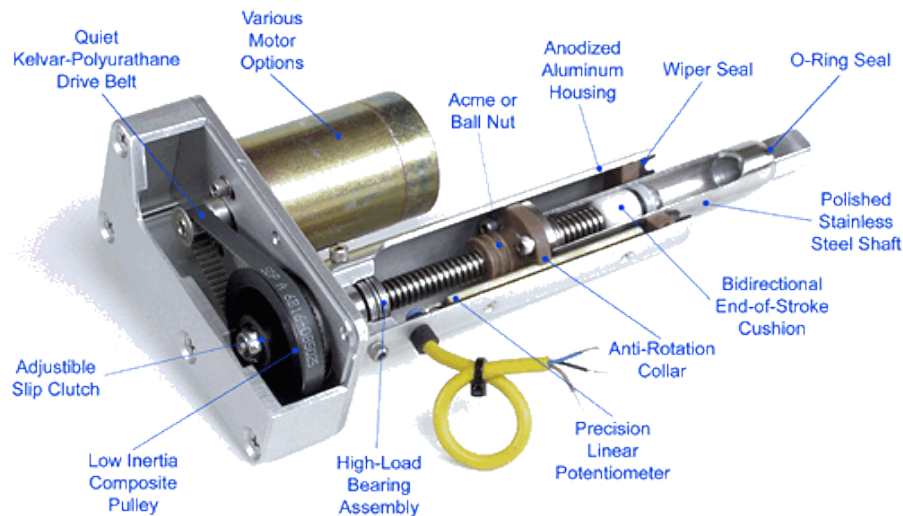

A linear actuator made by Ultramotion

Linear actuators are widely used in home solar tracking application since it is easy to control and relatively inexpensive. Horizontal rotation can be achieved by mounting the base of the linear actuator on a tracker frame and the stroke connected to the solar panels. Linear actuators with varying stroke length and gear ratio (which determines the maximum thrust) can be purchased.

In many cases, both the linear actuator and the slewing drive are used to achieve dual axis tracking.
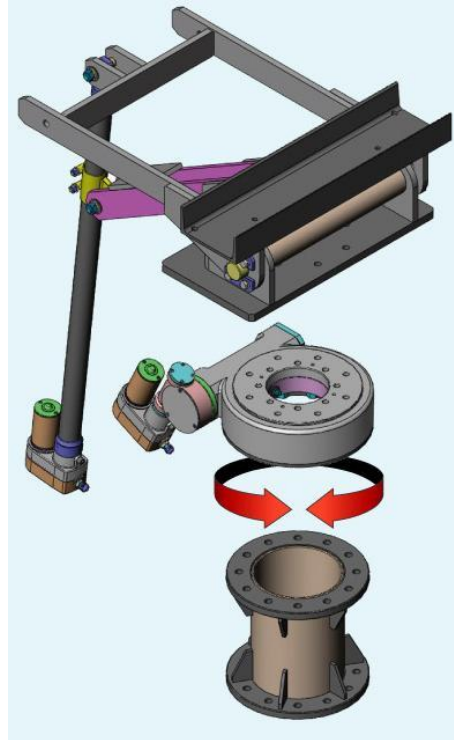
A complete dual axis tracing system made by Sunflower Energy

[http://www.sunflowerenergyinc.com/GSS-Slewing-Drive.html]

2.5. *Future potential of solar trackers --> any use and if yes for what kind of use? MELANIE*

Future prospects:

The debate on solar energy production is a controversial one with concern about the efficiency, reliability and above all the commercial feasibility pertaining to the investment cost and grid parity of the system. Government subsidies have encouraged R&D in the development of PV solar system as the alternative to natural gas which is the biggest competitor in the production of electricity. However, skeptics are still dubious about solar power potential. In the limit that solar power may take another century to be the sole provider of electricity for the whole world, there are great expectations that it will be able to provide for at least … To complete!!!

1. **Efficiency**

   The efficiency of Dual-Axis PV solar system as compared to that of the fixed Solar system is at 20-35% efficiency under ideal conditions, while Mousazadeh et al. found that solar tracking could potentially double the efficiency under ideal conditions [E]. With sunlight variations due to the earth rotation and cloud cover, the average electrical power obtainable over a year would be about 20% of its peak wattage [E]. Another published article conducted in Jordan have reported increases in power gain of up to 43.87% in Dual-Axis tracking as compared to 15.69% for North-South tracking [D].

   Despite the fact that solar cells can last 20 to 25 years, output power is reported to decline by approximately 0.5 percent per year even with periodical maintenance to keep peak efficiency.

This implies that by the end of 20 years they will only produce a maximum of 80 percent of their rated capacity [A] which will amount to only 16% of their peak wattage under ideal conditions. This will be equivalent to …find value

2. **Reliability**

One of the biggest advantages of the conversion of solar energy to electricity via photovoltaic means is the autonomy of each solar panel collector [C]. Most solar panels are individually fused so that in the event of a defective panel, it will not affect the other panels and can be easily replaced without affecting the whole connected system.

Despite the long-term benefits of solar energy, the biggest problems remain the low energy generation and the energy storage ability. To complete!!!

3. **Investment capital and pay back. Grid parity**

Currently, subsidized solar energy costs between $0.22 per kilowatt-hour and $0.30 per kilowatt-hour, according to independent analyses. By contrast, the average cost of electricity nationwide is expected to remain roughly $0.11 per kilowatt-hour through 2015, according to an August 2010 White House report. [A]…to complete!!!!

4. **Feasibility**

The most important concern for investing in solar energy production is the time required for the subsidies to remain in place for these systems to be autonomously profitable and feasible. The fact that the price point of grid parity depends on a number of variables such as the amount of sunlight an area receives, the orientation of the solar array, whether the solar arrays are fixed or track the sun, construction costs, rate structure and financing options, resulted in significance difference in breakeven costs by more than a factor of 10 [A]. Nevertheless, grid disparity was reached in Hawaii where the average price for electricity was …[A]. Arizona is another location which receives abundant sunlight and where grid parity would have been reached if not for its limited transmission access and low electricity prices [A].

Despite these economic factors as well as practical concerns, Solar power could become the most important power source if the technology catches up to increase the efficiency of the system…to complete!!!

[A] H. Sterling Burnett. Solar Power Prospects. *National Center for Policy Analysis*; Policy Report No. 334 May (2011) http://www.ncpa.org/pdfs/st334.pdf

[B] The Prospects for Cost-Competitive Solar PV Power," a new working paper by Professor Stefan Reichelstein http://www.gsb.stanford.edu/news/headlines/Reichelstein-solar-2012.html

[C] [http://iopscience.iop.org/0150-536X/11/6/010/pdf/0150-536X_11_6_010.pdf

[D] The effect of using sun tracking systems on the voltage–current characteristics and power generation of flat plate photovoltaics Salah Abdallah

[E] A review of principle and sun-tracking methods for maximizing solar system output

3. **Goal statement**

4. **Design Specification – Melanie**

Let's just put a general design specification (those that are important) here. We can explain in detail in the next section.(Myo)

The design specifications for the STS444 are based on specifications set by the FDE and additional specifications that pertain to the functional model as listed:

1. The functional model should be a three-piece assembly that could be disassembled into the panel, frame support and base

2. The three disassembled parts should fit within a design envelop of 62" x 32" x 12" for storage and transportation

3. The function model should be able to assembled or disassembled within 1 minute and should be easily transported by one person

4. The total weight must be less than 80 lb

5. The panel should be able to rotate a full 360 degrees around the vertical axis

6. The panel should be able to tilt a maximum of 80 degrees with the horizontal axis

7. The model should be able to demonstrate snow removal simulation, solar tracking up to ±5 degree accuracy, and bracing in windy conditions to reduce drag forces.

8. The model should receive all necessary power from the 110V wall socket

9. The prototype sensors should respond to external stimuli for wind and sun simulation

10. Parts used should be easily obtained and compatible with all assembly parts used

11. The prototype must be designed so that all parts have a finite life cycle of …

12. The prototype must be easy to troubleshoot and easily assembled by a trained mechanic

13. Welds should not be present in any moving parts and must contain no attachments except fasteners

14. Other ECE task specs

5. Design Description – Melanie/Myo

(Myo)

The purpose of the functional model is to be able to demonstrate to the FDE customers how the large scale model (STS44) is going to work. The model should be small enough to fit in the back of a car and light and mobile enough to be transported by a single person into a meeting room. Since the model would be seen by future customers of FDE, it should include all the features of the STS444 and must also look appealing.

As shown in figure *, the functional model assembly is composed of three main parts: the photovoltaic panel, the support frame and the base. A panel with the dimension 32" x 62" is provided to the team by FDE, so all the other parts are designed to conform to the size and weight of the panel.
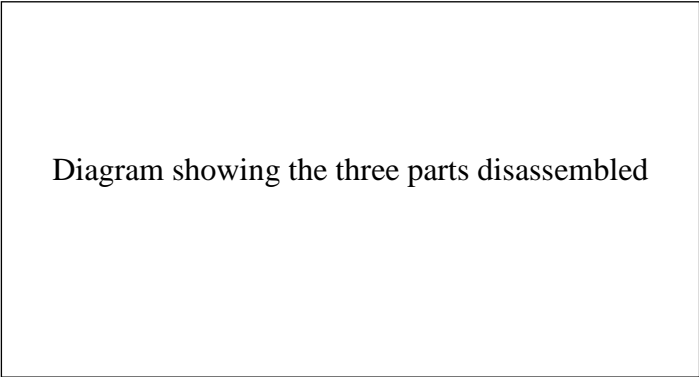
Diagram showing the three parts disassembled

Before any parts of the model are designed, extensive research must be carried out to find what kinds of parts and materials are available on the market, and preferably online. Websites like AmazonSupply, McMaster-Carr, and SDP/SI are used to find parts that might be useful for the model.

(Melanie)

Clearance, dimensions, components, materials,

The prototype design assembly is composed of the PV collector, the support frame and the base. A system of linear actuator and slewing gear are used to rotate the PV panel in both polar and azimuth angles which are controlled by …ECE… Some of the mechanical and electrical components were both manufactured and purchased as described in the following section.

5.1. Concepts

5.1.1. Linkages

The most commonly used type of linkage for elevation angle changes in PV collector is roughly that of a fourbar linkage with the linear actuator comprising the second and third linkages connected by a slider (Fig. A). Link 4 and Link 2 are pivoted to ground while Link 2 and Link 3 are connected by an assumed frictionless slider. Link 2 is assumed to act as the input link and is driven at a constant speed of … During this motion the combined length of Links 2 and 3 decrease and Link 4 is pivoted at ground in a clockwise direction through a maximum angle of 80 degrees.

Link 4 – PV collector

μ

Link 1
Grounded

Link 3

Linear
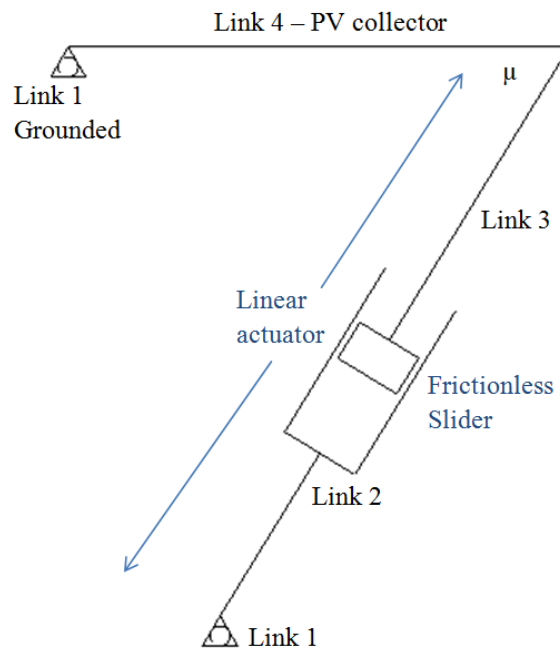actuator

Frictionless
Slider

Link 2

Link 1

Figure A. Schematic of linkage equivalence of the linear actuator system connected to the PV collector and the frame support showing the Links 1 – 4 and transmission angle μ.

5.1.2. Linear actuator positioning

The position of the linear actuator attachment points are defined by the size and stroke length of the linear actuator, the maximum angle of tilt and the transmission angle. The exact location for the position of the linear actuator can be found by graphical and analytical methods.

Ideally the linear actuator would be in compression when carrying the highest load, that is, when the panel is being pushed up from a tilted position to the horizontal position. From a material engineering point of view, the microvoids and shear bands tend to form in relatively brittle materials in tension which limit the ability of the material to undergo strain. Though in such a small scale system as the functional prototype sudden fracture is not likely to cause any damage, on the STS 444 system, creep is one of the most critical material behavior to anticipate failure. This is why keeping the linear actuator in compression is so important.

Selection of linear actuator

Cost & performance: same cost & same velocity (2 inch/sec or 0.05m/s)

Capacity: all have maximum weight of 25+ lbs (pound mass) = 800lbf/3560N

Size: the longer the stroke the heavier the linear actuator (by how much?)

Limiting condition: Max force and stress in linear actuator when extended at maximum length

Dimensional limitation
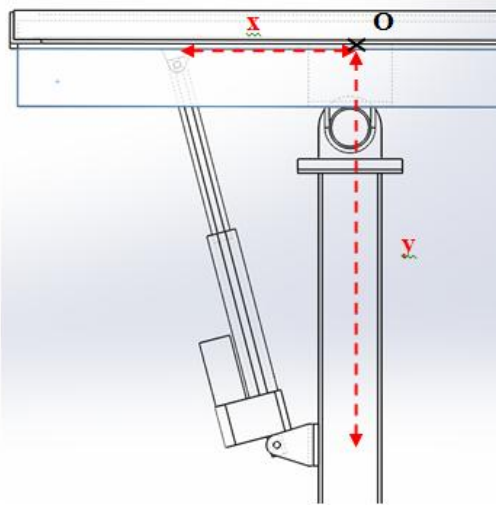
Attachment range for linear actuator:

Stroke	A1(ext)	A2 (retr)	xy/in^2
1.96	9.64"	7.68"	17.23
3.93	13.62"	9.69"	46.51
5.90	17.59"	11.69"	87.71
7.87	21.57"	13.70"	140.93
9.94	25.65"	15.71"	208.73
11.81	29.53"	17.72"	283.32

Note that $x \leq r = 15.9"$ and $y \leq H = 27.1"$

5.2. Iterations:

5.2.1. Iteration 1
The first positioning iteration was…

Graph of y (f(x), g(x), h(x)…) against x distance from center O

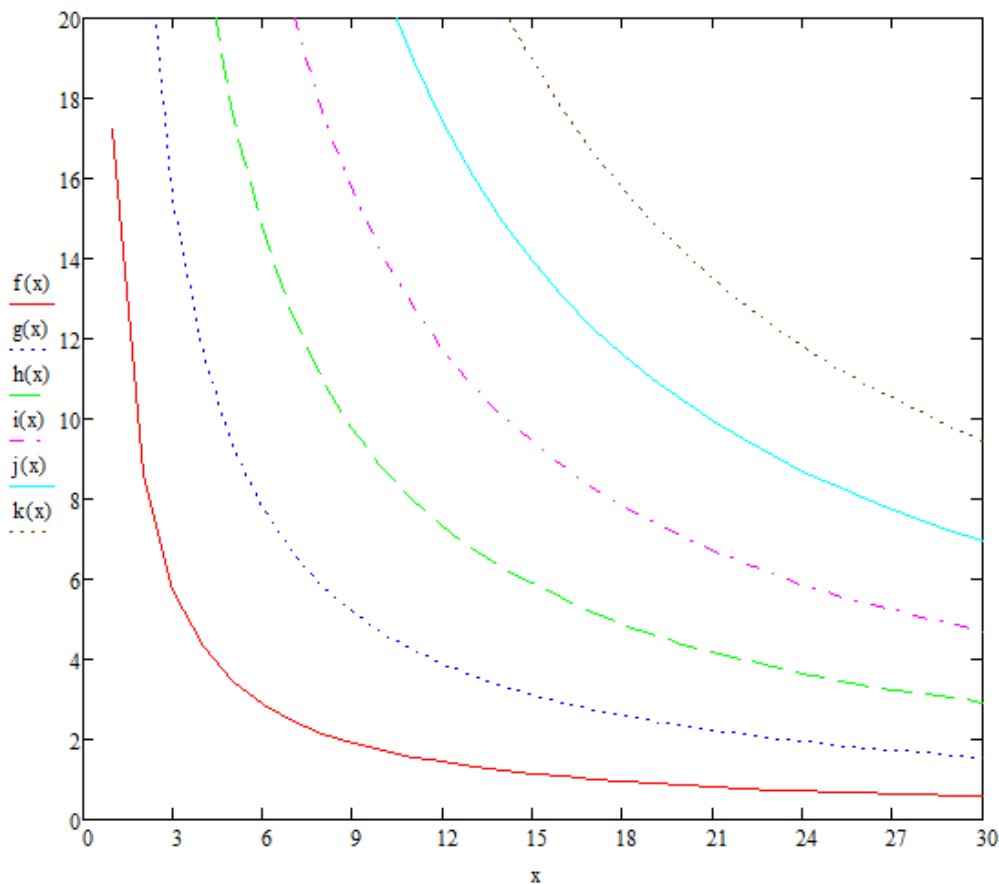$$f(x) := \frac{17.23}{x} \qquad x := 0, 1 .. 50$$

$$g(x) := \frac{46.51}{x}$$

$$h(x) := \frac{87.71}{x}$$

$$i(x) := \frac{140.93}{x}$$

$$j(x) := \frac{208.73}{x}$$

$$k(x) := \frac{283.32}{x}$$

Positioning Limitation

1. The dimension ranges were calculated only at the different extreme positions and dynamic motions were not taken into consideration
2. Rotation point taken in the middle of panel when in reality pivot point is found some distance below
3. Attachment points of linear actuator on panel and beam were taken to be lying right onto the mid-axis. Optimum position of the attachment points might not be lying on the vertical & horizontal axes.

5.2.2. Iteration 2:
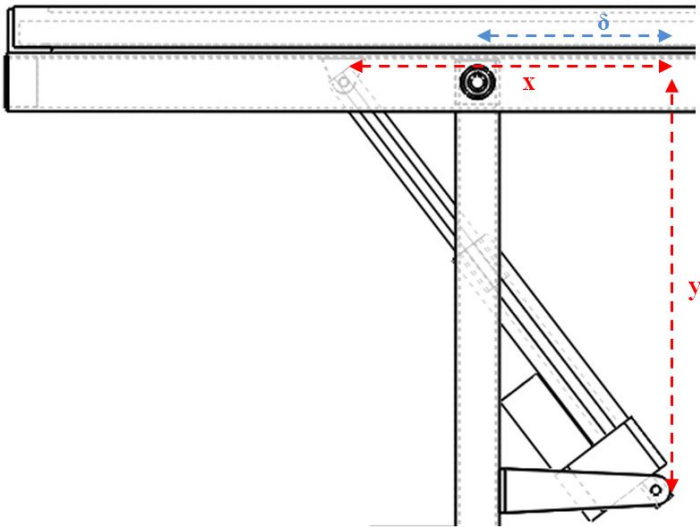
The analytical method produced two possible solutions for each specific length of linear actuator which were checked graphically and the transmission angles were subsequently compared for both solutions.

Analytical method

The following conditions applied are the maximum tilt of the collector from the horizontal at 80 degrees, extended length *a*, retracted length *b* of the linear actuator and the stroke length *l* as per the manufacturer's specifications [http://www.servocity.com/html/115_lbs__thrust__linear_actuat.html] and as defined by Table A.

Table A. Definition of variable terms used to calculate the optimum position of the linear actuator

| Term	Definition
a	Extended length of linear actuator
b	Retracted length of linear actuator
l	Stroke length of linear actuator (b-a)
x	horizontal distance from bottom to upper attachment points of the linear actuator when completely extended
y	vertical distance from bottom to upper attachment points of the linear actuator when completely extended
δ	Offset distance of linear actuator attachment point on the collector to the pivot of the collector on the frame support.
θ	Angle between panel and vertical axis
z_b	Horizontal distance between the centers of the two vertical frame support beam
D	Diameter of outer slewing gear
d	Distance between centers of outer slewing gear and pinion
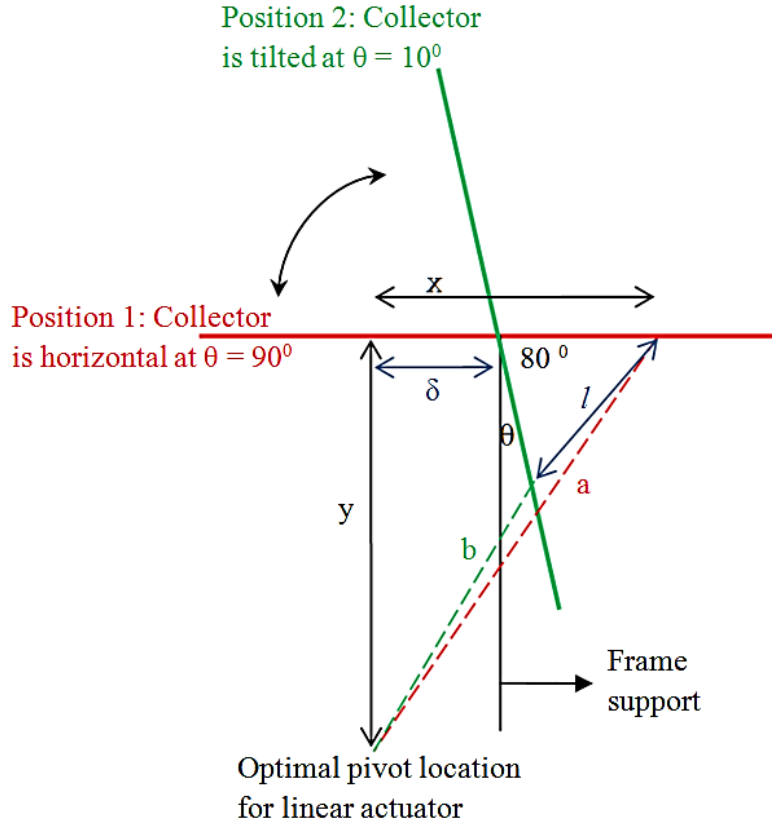
Figure B. Schematic of the defined variables of the collector and frame support assembly at the two extreme positions which are defined by angle θ, extended a, retracted length b, stroke length l and offset distance δ.

The first step is to find the offset distance δ depending on the stroke length l as calculated by Equation 1

Equation 1 $\qquad\qquad l^2 = 2(x - \delta)^2 - 2(x - \delta)\cos 80$

From Figure B, two solutions x_1/y_1 and x_2/y_2 are obtained from the two simultaneous Equations 2 and 3 using the value of δ obtained from Equation 1:
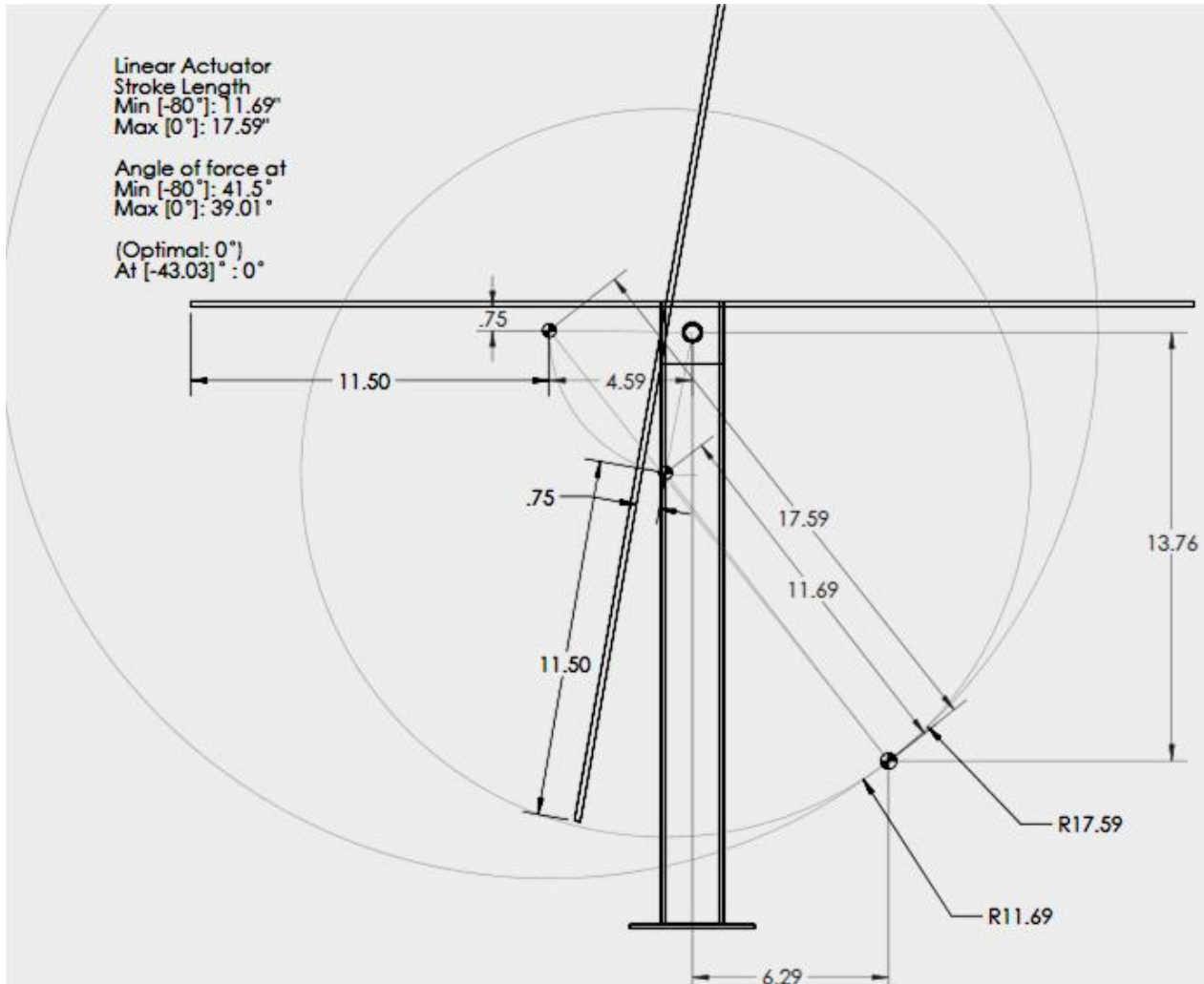
Equation 2 $\qquad\qquad x^2 + y^2 = a^2$

Equation 3 $\qquad\qquad [\delta + (x - \delta)\cos 10]^2 + [y - (x - \delta)\sin 10]^2 = b^2$

Solutions for each of the five different types of linear actuator available from the vendor's website were calculated in Appendix A.

The 5.90 inch stroke length linear actuator was chosen for its compactness and minimum transmission angle at greater than 40 degrees.

By graphical method

The two analytical solutions obtained for the 5.90 inch stroke length linear actuator were drawn graphically and the corresponding transmission angles μ were measured at each location. A radius of 4.59 inch was drawn on the horizontal panel extended through 80 degrees to the panel tilting at that angle. With a 5.90 inch stroke length, x and y at 10.70 inches and 13.96 inches respectively, the minimum transmission angle was 52 degrees as compared to a transmission angle of 10 (to check) degrees at the second location.

The closer the linear actuator center of gravity is to the center of gravity of the support frame, the more stable the assembly will be which will in turn require a smaller surface area for the base. The second solution for x and y would have resulted in a distance difference of…from the two centers of gravity which cause instability in addition to the angular momentum from the moving parts.

5.2.3. Iteration 3
To complete!! Landing gear 6-bar mechanism
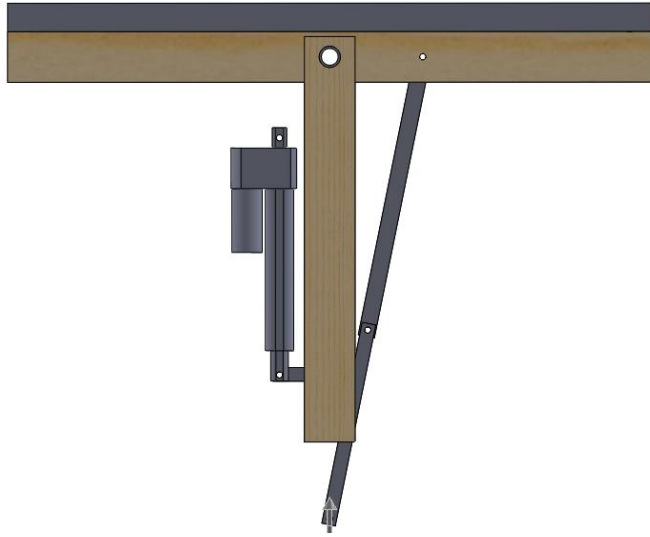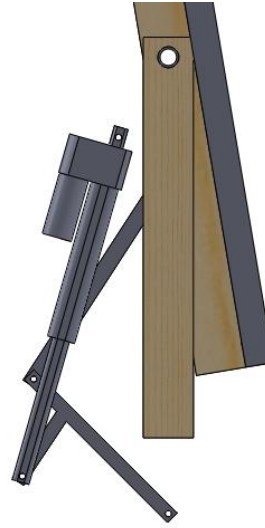
Six-bar Mechanism   2 four-bar mechanism combination
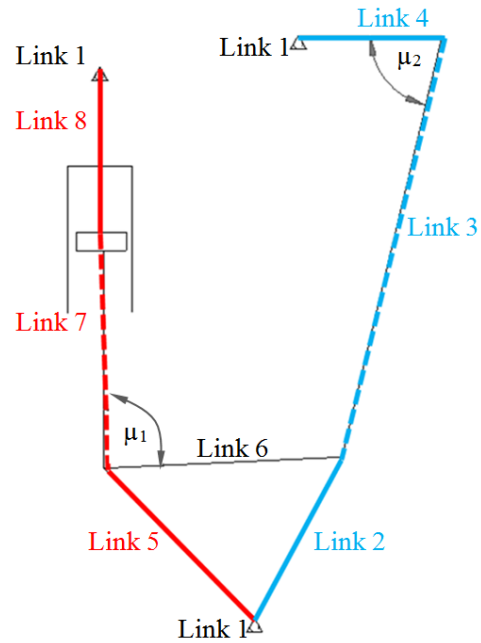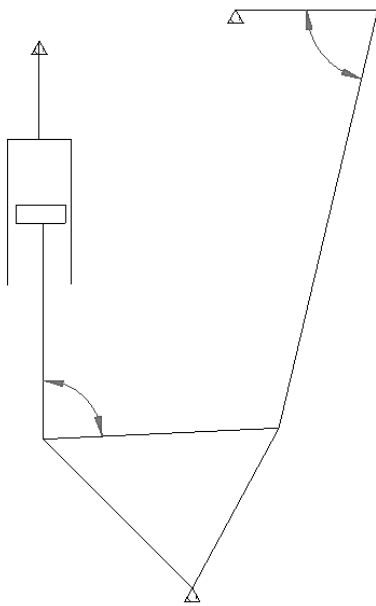
Figure DS. Drawing of the Sixbar mechanism broken down into two Fourbar mechanism – "LA_Fourbar" (Red) and "PV_Fourbar" (blue).

This iteration consisted of a Sixbar linkage which can be broken down into two Fourbar mechanism connected with a ternary link.

For the determination of the lengths, the right hand side Fourbar mechanism "PV_Fourbar" (Fig. DS – blue), is analyzed first through *Linkages* program by varying the amount of lengths while keeping in mind the transmission angle to be greater than 40 degrees minimum (Fig.GH.).
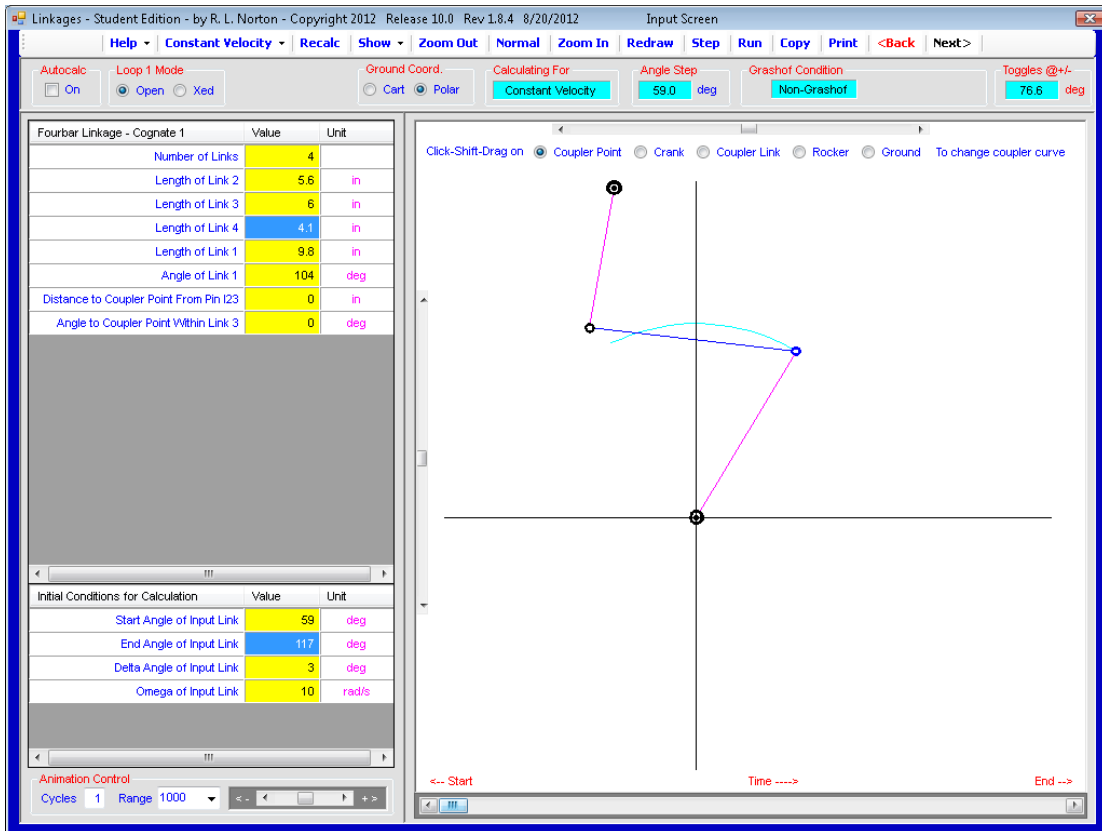

Figure GH. Lengths of Fourbar "PV_Fourbar" mechanism as calculated in *Linkages* program.

Transmission angle as calculated ranged from 44.4 degrees to 86.5 degrees which was acceptable since it was higher than the minimum 40 degrees and varied to within $\pm$ 50 degrees (Fig. JK)
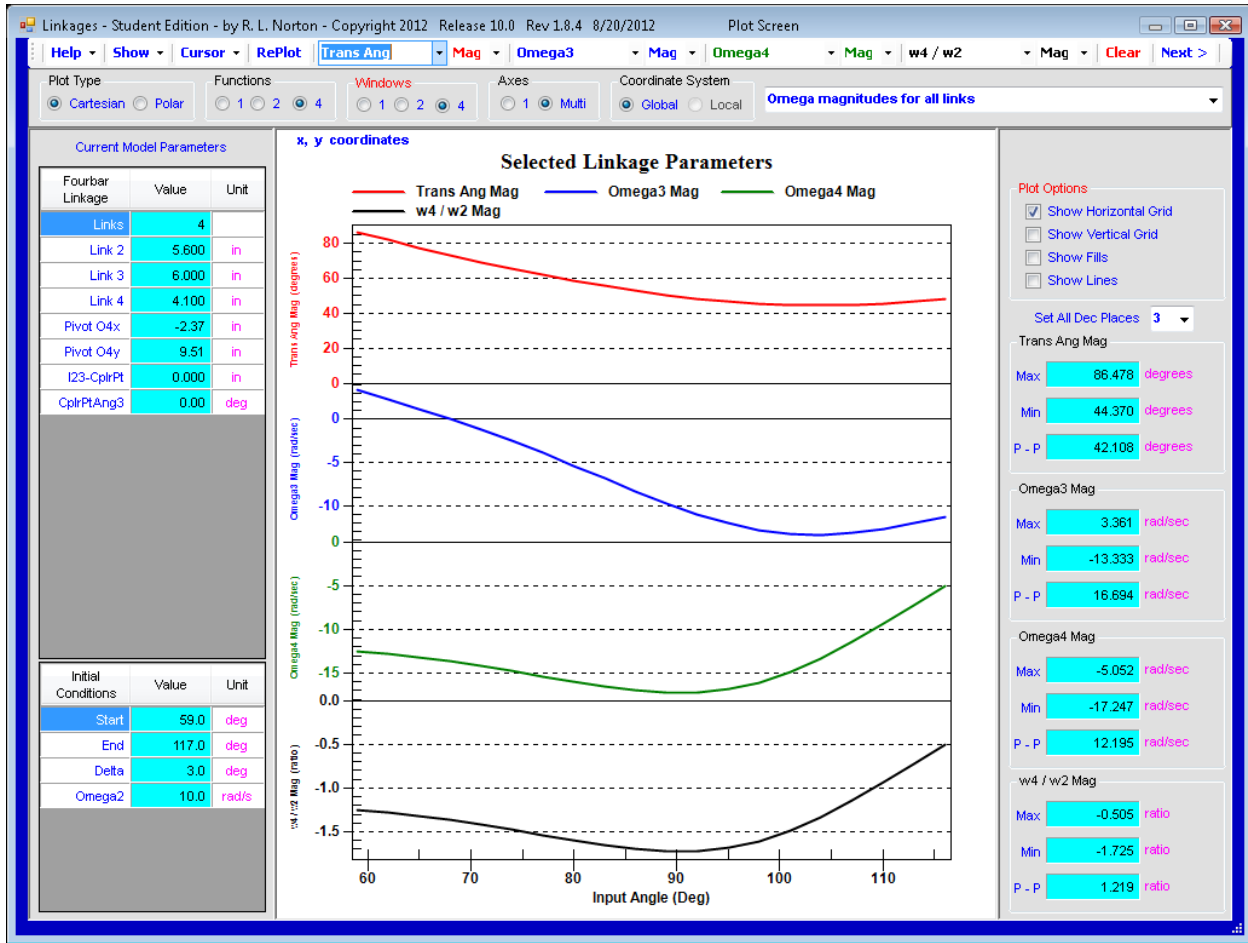
Figure JK. Transmission angle μ_2 ranging from 44.4 degrees to 86.5 degrees as plotted in *Linkages* program for the "PV_Fourbar".

As an acceptable range for linkage lengths for "PV_Foubar" mechanism, the linear actuator length, limited by the retracted and extended lengths, is added to optimize the system for a maximum tilting of 80 degrees and all transmission angles μ_1 and μ_2 at more than 40 degrees. The optimized design is found by graphical method…The size of the mechanism is scaled depending on the stroke length of the chosen linear actuator which in our case will be the 15 cm (5.90 inch) stroke length as provided by manufacturer [ref]

Ideally the height of the mechanism will be slightly more than half the width of the PV collector for complete tilting without any obstruction. Measurement of transmission angle μ_1 yielded 40 degrees and 86 degrees approximately at the two extreme positions (Fig. KL).
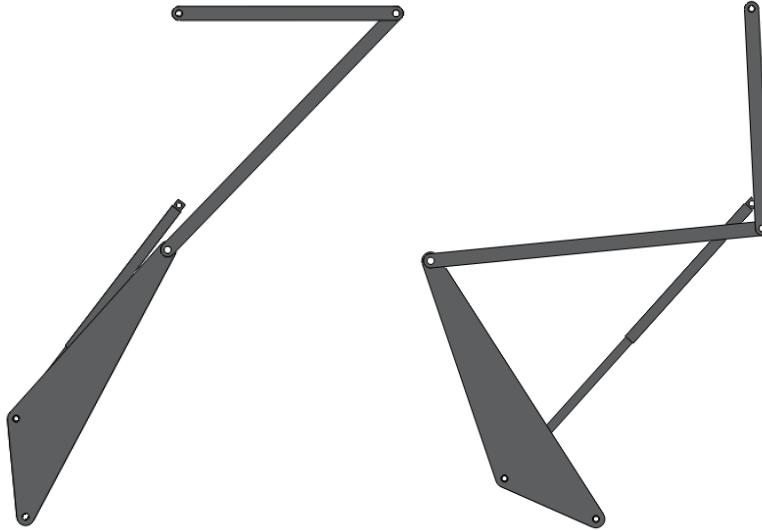
Figure KL. Solidworks Model of the Sixbar mechanism showing the two extreme positions at θ = 90 degrees (left) and θ = 10 degrees (left). Transmission angles μ_1 and μ_2 were 40 degrees and 86 degrees at horizontal position (left) and 44.4 degrees and 86.5 degrees at tilted position (right) respectively.

5.2.4. *Slew gear dimension*
!!!Find transmission angle, pressure angle and backlash…etc

5.3. Static force analysis

5.3.1. *Design Iteration 1*
From a preliminary measurement of the transmission angle for Design Iteration 1, since the transmission angle dropped lower than 40 degrees, all analysis thereon will be disregarded and not reported.

5.3.2. Design iteration 2

Static reaction forces at the different point of contact are tabulate in Table 1.

Table 1. Static reaction forces at all points of contact on the functional model

| Parameter	Definition	Quantity
Weight/N		
W	Weight of the PV collector	160
w_{la}	Weight of the linear actuator	12.0
w_b	Weight of the beam (bearing??)	1.00
w_{tt}	Weight of the turn-table	4.20
w_p	Weight of the pinion (this includes the motor weight)	3.00
w_B	Weight of the base	??
Length/mm		
l_{ext}	Extended length of linear actuator	446.8
l_{ret}	Retracted length of linear actuator	296.9
l	Stroke length of linear actuator (b-a)	149.9
a	Horizontal distance of CG of linear actuator from bottom end	38.83
b	Vertical distance of CG of linear actuator from bottom end	118.2
x	horizontal distance from bottom to upper attachment points of the linear actuator when completely extended	116.5
y	vertical distance from bottom to upper attachment points of the linear actuator when completely extended	354.6
δ	Offset distance of linear actuator attachment point on the collector to the pivot of the collector on the frame support.	155.2
z_b	Horizontal distance between the centers of the two vertical frame support beam	
D	Diameter of outer slewing gear	
Angle/degree		
θ	Angle between panel and vertical axis	10.0 – 90.0
Angular Velocity/ rad.s^{-1}		
Angular Acceleration/		

Table..Static reaction force equations, magnitudes and directions as obtained by calculation and on Solidworks at the two extreme positions

Force	Theoretical Forces formula	Relation	Direction	Absolute magnitude		Solidworks	
				Calculated			
				θ=10	θ=90		
R_{Ox}	$w_{la}tan\theta\left(\dfrac{a}{x+ytan\theta}\right)$	R_{Ax}		0.460	0		
R_{Oy}	$W+w_{la}(\dfrac{a}{x+ytan\theta})$	$W-R_{Ay}$		157.4	160		
R_{Ax}	$w_{la}tan\theta\left(\dfrac{a}{x+ytan\theta}\right)$	$R_{Ay}tan\theta$		0.460	0		
R_{Ay}	$-w_{la}(\dfrac{a}{x+ytan\theta})$	$R_{By}-w_{la}$		2.600	0		
R_{Bx}	$-w_{la}tan\theta\left(\dfrac{a}{x+ytan\theta}\right)$	$-R_{Ax}$		0.460	0		
R_{By}	$w_{la}(1-\dfrac{a}{x+ytan\theta})$	R_{By}		9.400	12.00		
R_{Cx}	$0,\dfrac{R_{By}}{R_{Bx}}=\dfrac{y}{\delta}$	$\dfrac{-R_{Bx}-R_{Ox},}{\delta R_{By}-yR_{Bx}}$ L_b		0	0		
R_{Cy}	$W+w_{la}+w_b$	$R_{Oy}+R_{By}+w_b$		173.0	173		
R_{Cz}	0	0		0	0		
R_{Dx}	0	0		0	0		
R_{Dy}	$\dfrac{W+w_{la}+w_b+w_{tt}}{2}$	$\dfrac{R_{Cy}+w_{tt}}{2}$		88.60	88.60		
R_{Ex}	0	R_{Cx}		0	0		
R_{Ey}	0	0		0	0		
R_{Fx}	0	R_{Cx},R_{Ex}		0	0		
R_{Fy}	w_p	w_p		3.000	3.000		
R_G	$W+w_{la}+w_b+w_p+w_{tt}+w_B$	Total weight		180.2 $+w_B$	180.2 $+w_B$		

!!!Find shear stresses/forces in beam…

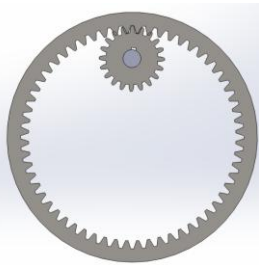### *1.3.3. Iteration 3*
!!!To complete!!!!!
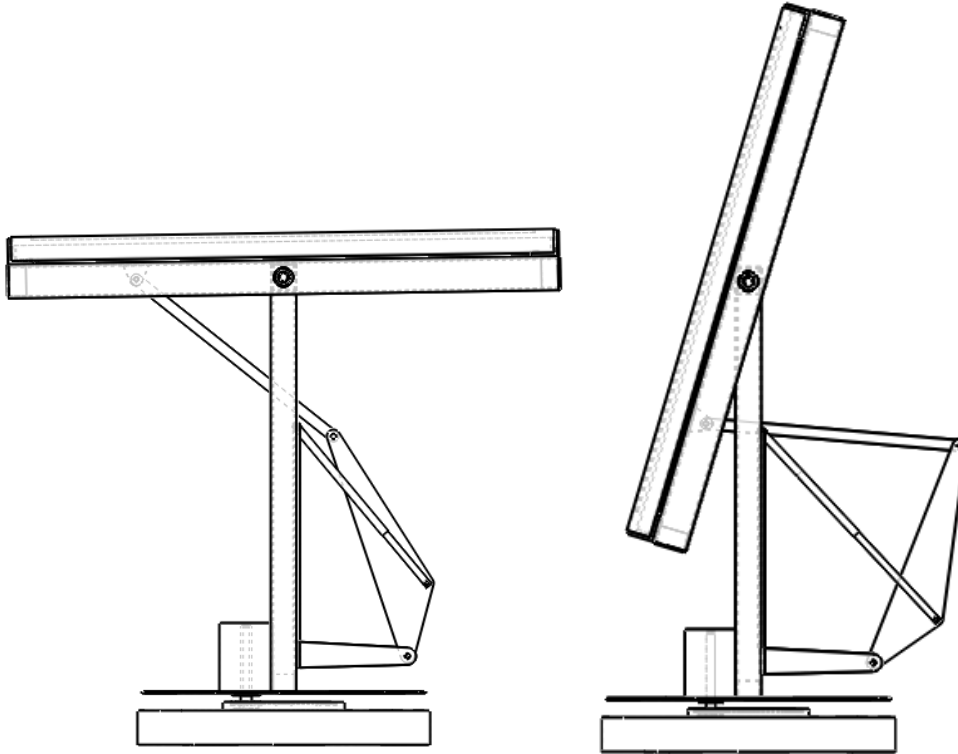
1.3.4. Gear analysis:
Type: internal spur gear

Path: involute curve

$$Z = \sqrt{(r_p + a_p)^2 - (r_p cos\varphi)^2} + \sqrt{(r_g + a_g)^2 - (r_g cos\varphi)^2} - C sin\varphi$$

Most common angle for pressure angle = 20 degrees, r_p = 5 cm and r_g = 15 cm

Contact ratio: $m_p = \frac{p_d Z}{\pi cos\varphi}$ where p_d = base pitch/diametral pitch

$$p_d = \frac{\pi}{p_c} \qquad p_c = \frac{\pi d}{N},$$ N= number of teeth, d = pitch diameter

Find transmission angle =

http://accessengineeringlibrary.com/browse/handbook-of-mechanical-engineering-calculations-second-edition

 reported efficiency of spur gears = 99-98%
[experimental investigation of spur gear efficiency. Petry-Johnson. Ohio state university]
[ref: **Prediction of Mechanical Efficiency of Parallel-Axis Gear Pairs. Xu et al. Journal of Mechanical Design** JANUARY 2007, Vol. 129 / **59**]

Possible gear dimension: Pitch 16 in either 95 teeth or 20 teeth

Possible coefficient of friction:

5.4. Motion and Power Analysis

5.4.1. Design iteration 1:

Dynamic analysis unnecessary since transmission too low.

5.4.2. Design iteration 2:

Power (linear actuator)

Given azimuth rotation should be executed in less than 15 second (half cycle) and that model accelerated in 1 second only.

$t_a \leq 15$ s

$\omega_a \geq 80\pi/(180 \times 15)$ rad.s^{-1}

$\alpha_a \geq 80\pi/(180 \times 15 \times 1)$ rad.s^{-2}

Power needed for linear actuator to rotate the PV collector initially:

Theoretically $\qquad P_{la} \geq I\omega\alpha = 0.9511 \times \left(\frac{80\pi}{180 \times 15}\right)^2 \geq 0.008W$

Solidworks (based on linear velocity 0.00889 ms^{-1}) :

At $\theta = 17\ deg \rightarrow \quad P_{la} \geq F \times v = 7.85 \times 0.00889 \geq 0.07W$

At $\theta = 90\ deg \rightarrow \quad P_{la} \geq F \times v = 70 \times 0.00889 \geq 0.62W$

Power (gear)

Mass Moment of Inertia

Part	Mass m/kg	x/m	y/m	d/m	Mass moment of Inertia Equations
1. PV collector	16.05	1.580	0.808	n/a	$I_{zz} = \frac{1}{12}m(x^2 + y^2)$
2. (Vertical beam support) x2	0.610	0.038	0.038	0.176	$I_{zz} = I_o + m\bar{d}^2$ $I_{zz} = \frac{1}{12}m(x^2 + y^2) + m\bar{d}^2$
3. (Horizontal beam support) x2	0.970	0.025	0.817	0.218	$I_{zz} = I_o + m\bar{d}^2$ $I_{zz} = \frac{1}{12}m(x^2 + y^2) + m\bar{d}^2$
4. Horizontal Frame support	0.293	0.005	0.390	0.050	$I_{zz} = I_o + m\bar{d}^2$ $I_{zz} = \frac{1}{12}m(x^2 + y^2) + m\bar{d}^2$
5. Linear actuator	1.20	0.050	0.200	0.100	$I_{zz} = I_o + m\bar{d}^2$ $I_o = \frac{1}{2}\left(\frac{1}{2}mx^2 + \left[\frac{1}{4}mx^2 + \frac{1}{12}my^2\right]\right)$
6. Cross beams	0.823 0.152	0.051 0.051	0.508 0.260	n/a	$I_{zz} = \frac{1}{12}m(x^2 + y^2)$

7.	Circular base	0.490	0.150	n/a	n/a	$I_{zz} = \frac{1}{2}mx^2$

Part	Mass Moment of Inertia (I_{zz}/kgm^2)	
	Calculations	Solidworks
PV collector	4.2121	4.6618
(Vertical beam support) x2	0.0381	0.0004
(Horizontal beam support) x2	0.2002	0.1092
Horizontal Frame support	0.0044	0.0030
Linear actuator	0.0031	0.0050
Cross beams	0.0188	0.0208
Circular base	0.0055	0.0056
Total	**4.4822**	**4.8058**

Note:

1. In calculations of mass moment of inertia for PV collector, supporting welded beams were not taken into account unlike in the solidworks simulations

2. The vertical beams and horizontal beams calculations were an overestimate since in reality they were hollow while in the calculations they were treated as filled.

3. Center of gravity for linear actuator in calculations was placed one third of total length in all directions from the base

4. Mass moment of inertia for linear actuator in solidworks was taken when linear actuator was completely vertical with center of gravity at one third distance of total length in all directions from the base.

5. Both results for mass moment of inertia by calculation and solidworks simulations do not include miscellaneous items such as the electric box, bolts, screws and other items that will add slightly to the mass moment of inertia.

Given that polar rotation should be executed in less than thirty second and that model accelerated in 1 second only.

$t_p \leq 30$ s

$\omega_p \geq 2\pi/30$ rad.s^{-1}

$\alpha_p \geq 2\pi/30$ rad.s^{-2}

Power needed for gear to rotate the model initially:

$$P_g \geq I\omega\alpha = 5 \times \left(\frac{2\pi}{30}\right)^2 \geq 0.219W$$

Angular displacement

Angle modification to set relative starting angle at 9.79 degrees which is the starting position
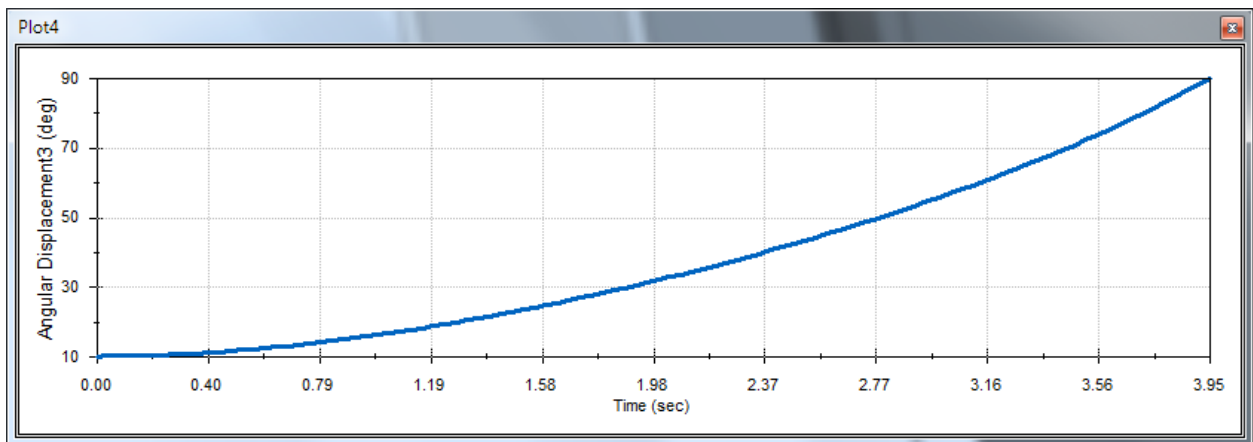

Figure GB Angular displacement with three points taken as (top vertex on horizontal beam, center point of bearing and vertex on vertical beam) with linear motor at 3 in/s. Incremental error in starting angle introduced due to points taken not being collinear within the same y-x plane. Therefore starting angle with panel completely tilted is slightly different from 10 degrees.

Modified plot in Figure GB to correct incremental error at the start

Graph of Angular Displacement against time

$y = 4.6544x^2 + 1.5962x + 9.85$
$R^2 = 0.9997$
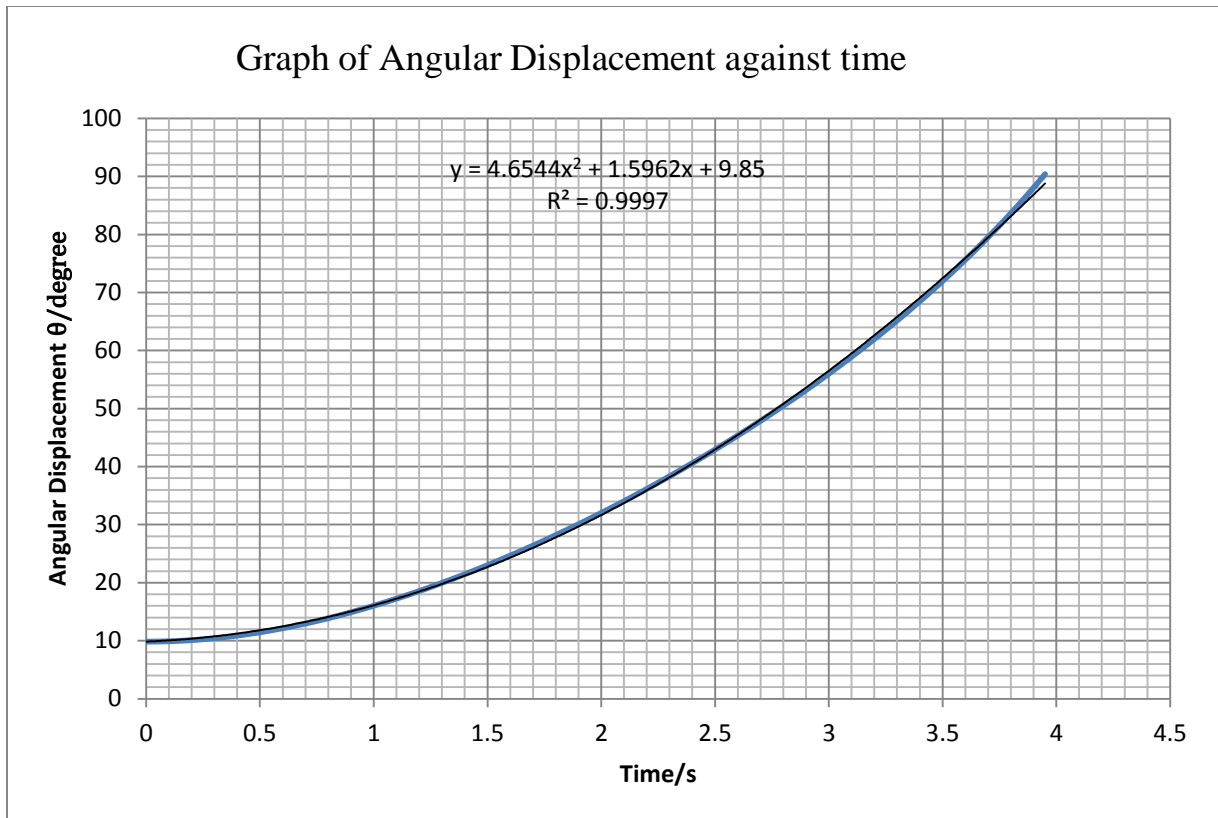
If the motion were to be considered linear, an R-squared error of 0.9921 would be obtained

$$\theta = 9.85e^{0.5712t}$$

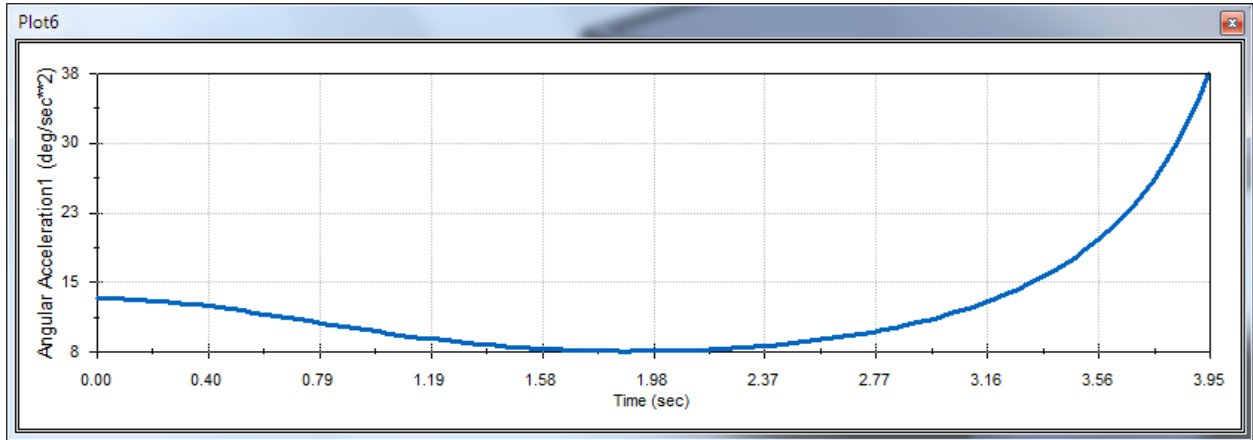As compared to the polynomial relation with an R-squared error of 0.9997

$$\theta = 4.6544t^2 + 1.5962t + 9.85$$

Angular velocity:
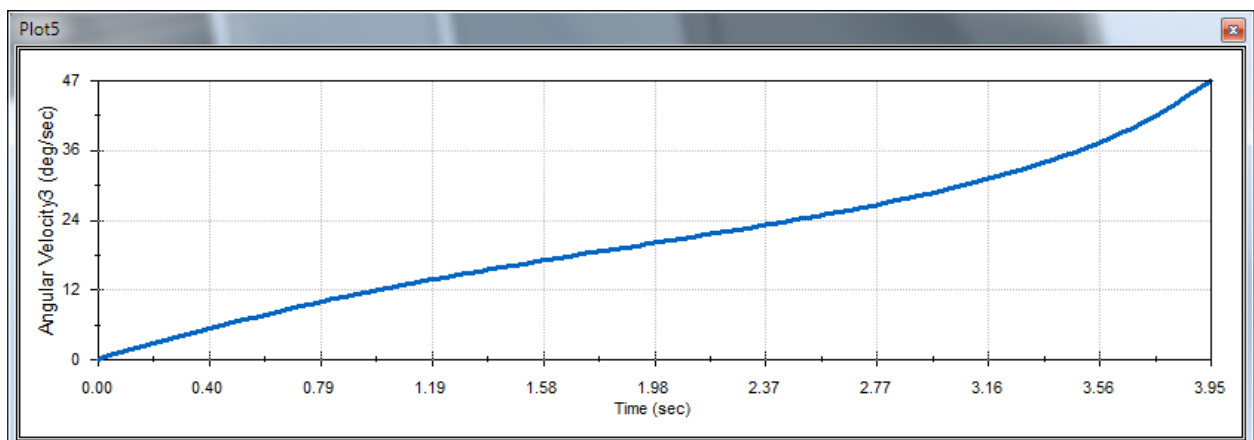
Angular velocity is almost zero at the start suggesting probably low transmission angles at the bearings. Maximum angular velocity reaches to about 47 degree/s

Angular acceleration

Dynamic Reaction Forces
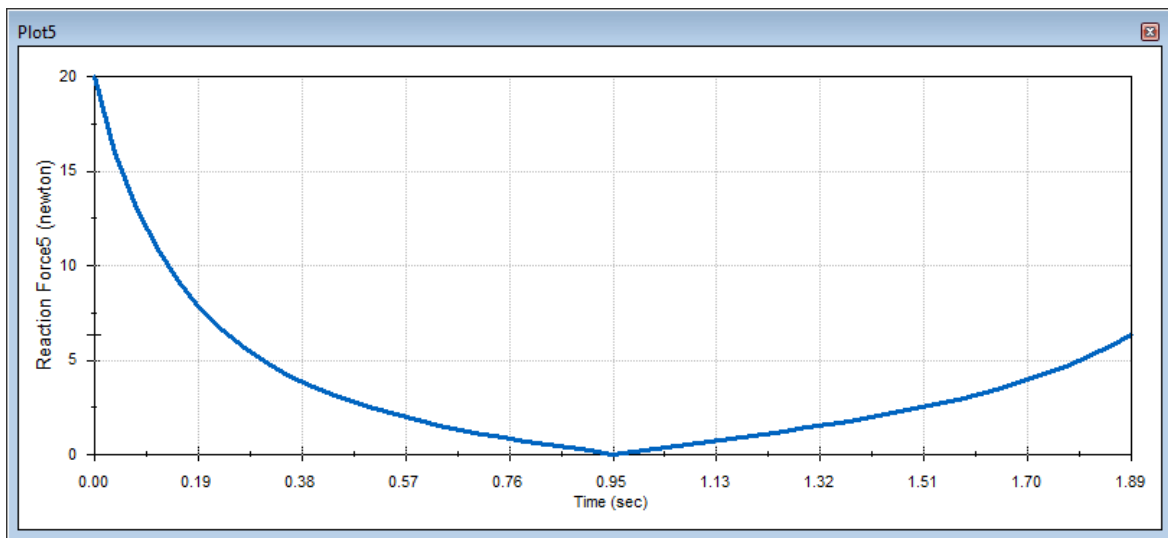
Figure ..Solidworks motion result plot of reaction forces at B (between bushing and shaft) against time for actuator speed of 3 inch/s. At 0.95 s reaction force is zero when angle between linear actuator and PV collector is at 90 degrees that is when transmission angle is maximum. (to check simulation with Planchard!!)

Motor torque
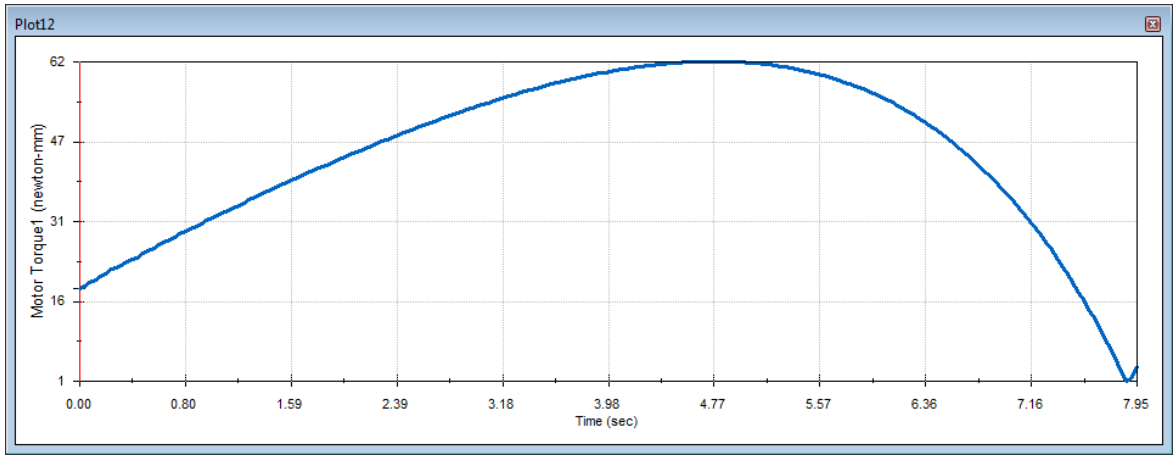
Figure ..Solidworks motion result plot of Motor Torque at gear with a combination of linear and rotary motion from Motor Torque (Gear) at 30 RPM and linear motor (linear actuator) at 2.54 cm/s. Each cycle last for approximately 8 seconds.
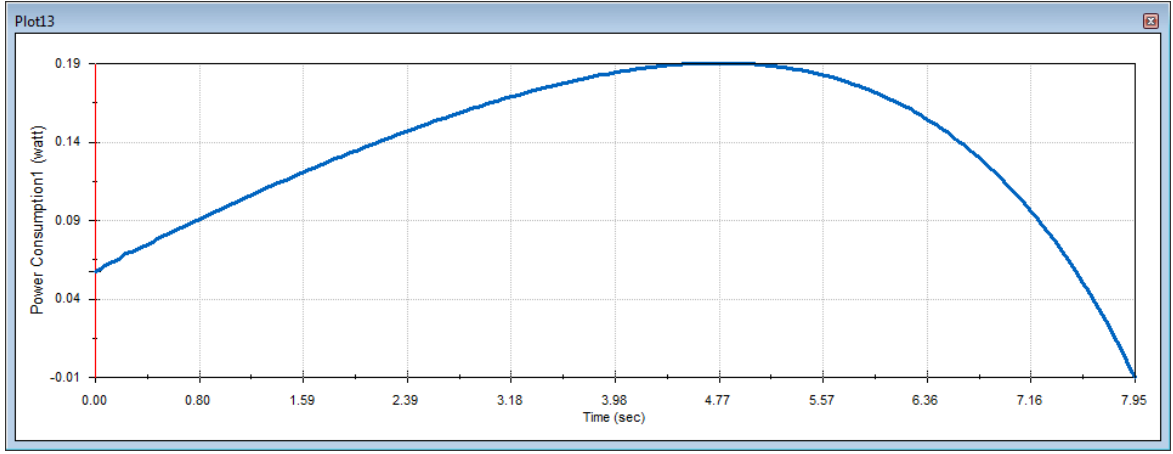
Power consumption by rotary motor

Figure ..Solidworks motion result plot of Power consumption by gear motor with a combination of linear and rotary motion from Motor Torque (Gear) at 30 RPM and linear motor (linear actuator) at 2.54 cm/s. Each cycle last for approximately 8 seconds.

5.4.3. Iteration 3:

The Design iteration 3 was analyzed under almost the same conditions as Design iteration 2 with the same panel and base except for the frame support mechanism. However for simplicity the linear actuator was not used but an equivalent simple link with the same weight and center of mass as the linear actuator used in the analysis of Design iteration 2.
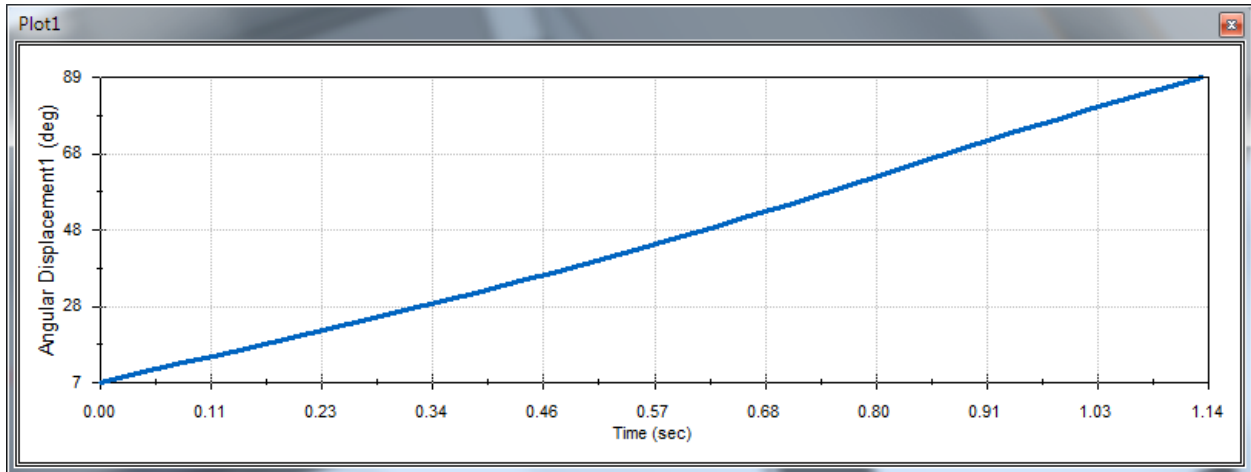
Figure…Angular displacement with three points taken as (top vertex on horizontal beam, center point of bearing and vertex on vertical beam) with linear motor at 3 in/s. Incremental error in starting angle introduced due to points taken not being collinear within the same y-x plane. Therefore starting angle with panel completely tilted is slightly different from 10 degrees.
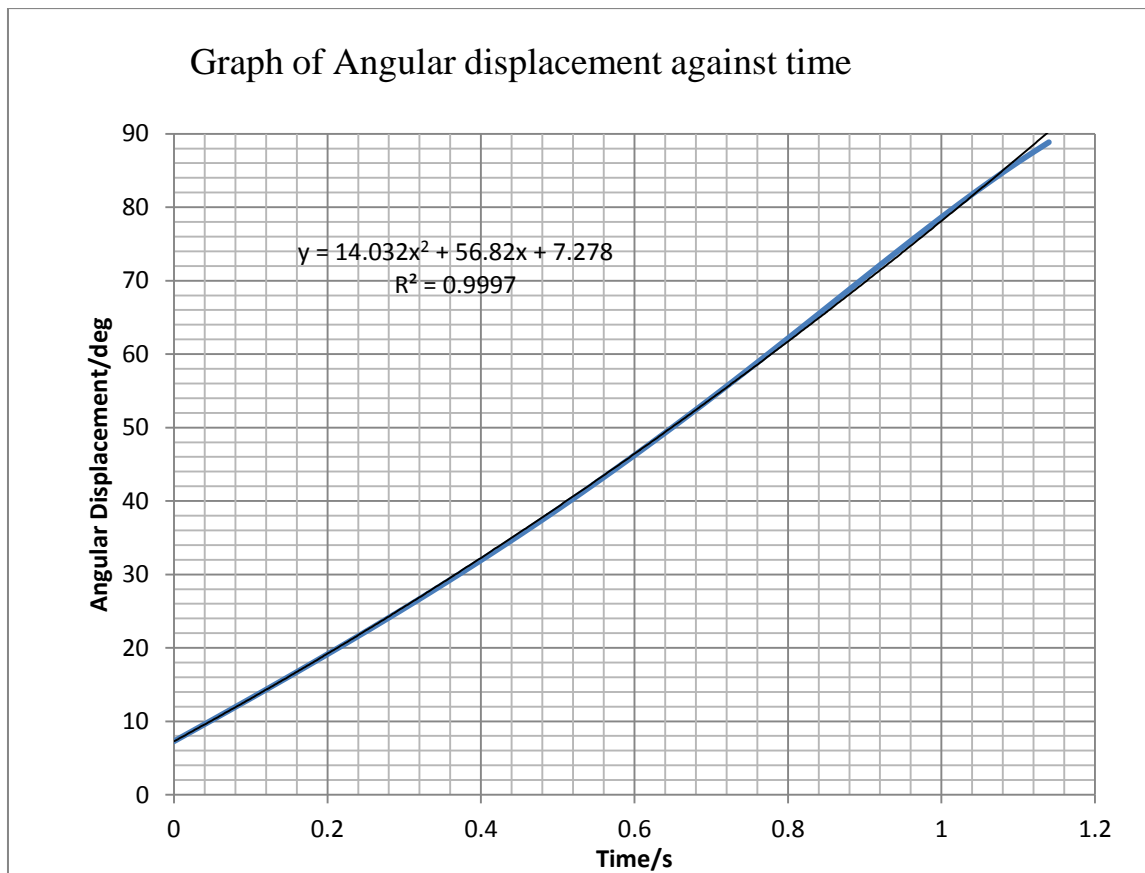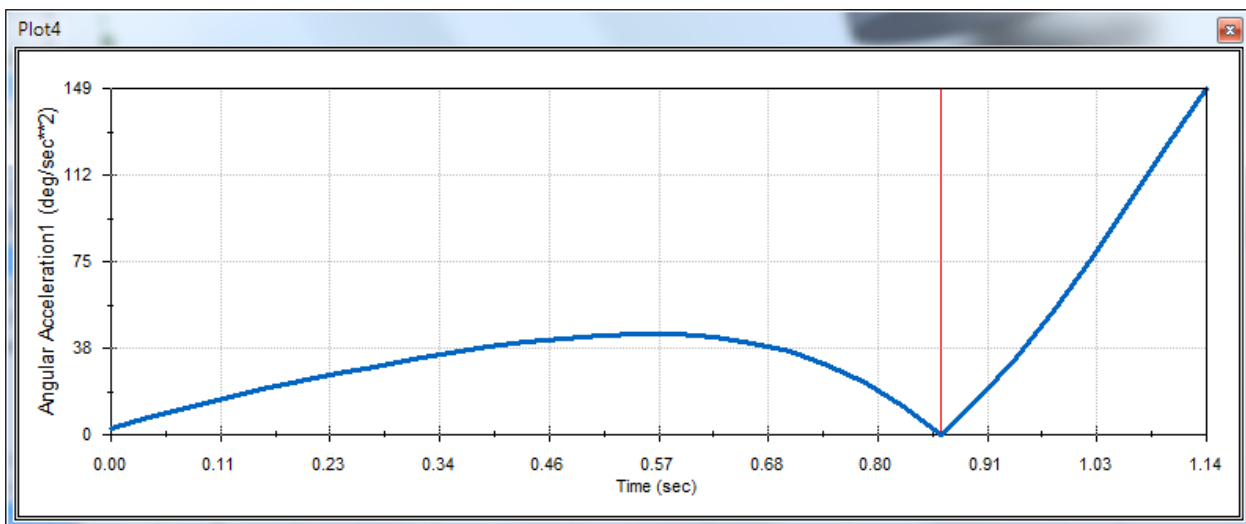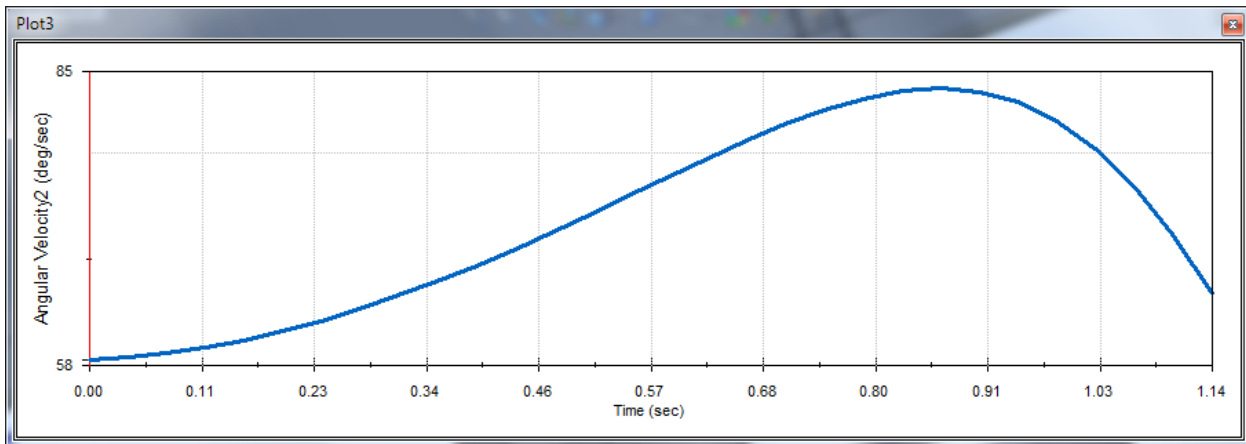

If the motion were to be considered linear, an R-squared error of 0.9926 would be obtained

$$\theta = 69.02t + 7.278$$

As compared to the polynomial relation with an R-squared error of 0.9997

$$\theta = 14.032t^2 + 56.82t + 7.278$$

Plot of angular velocity against time for Design iteration 3 at speed 76.2 cm/s

Summary

Table of comparison for motion analysis between Design iteration 2 and 3. Values for velocity at this first stage analysis is arbitrary. The worst case scenario at which the PV collector is rotating very fast is tested here in addition to soliworks simulations taking a long time to compute the motion. Later analysis would be limited to a whole cycle of 15 seconds or less for complete tilt.

Type of motion (speed of motor =	Design iteration 2 t = 3.95s	Design iteration 3 t = 1.14 s

76.2 cms⁻¹ or 3 in.s⁻¹)	min	max	min	max
Angular displacement (Deg/s)	Exponential		Almost linear	
Angular velocity (Deg/s)	0	47	58	64
Angular acceleration (Deg/s²)	0	38	0	149

5.4.4. Gear system

5.5. Sensors

5.5.1. Light Sensing Module

The light sensing module is the most important sensor in a solar tracker since it determines where the light is. Two light sensors, which make up a pair, will be placed at an angle and the signal produced from the sensors would be inputted into a microcontroller. For a dual-axis tracker, two pairs of light sensors would be used; one to determine the motion in one axis and another pair to detect the light in another axis. Any type of sensors that reacts to light intensity can be used. So a sensor testing experiment is carried out to compare different types of light sensors available to choose the best sensor for our application. One of the main constraints of this project is that the tracker would be used for demonstration in a room, tracking the light from an LED flashlight. So sensors that work well in the sun might not work for our case.

Electrical System

For our solar tracker to perform the way that is required, the electrical system needs careful consideration as it is an essential component. The electrical system needs to output precise, dependable control signals to the mechanical system and be as power efficient as possible in doing so.

Our initial design for the electrical system was to be purely analog. This was due to the intrinsic properties of an analog signal. Analog signals are continuous signals for which the voltage is a representation of some other time varying quantity, i.e., analogous to another time varying signal. Meaning, we can get a smooth continuous voltage difference from the changing angle of the sun with respect to the solar tracker. A digital system could still deliver this in principle, but differs from an analog signal by way of small fluctuations in the signal which can hold meaningful pieces of information, i.e., digital circuits lose small pieces of information do to the principle of sampling. No matter how many pieces of information are sampled per second, it does not compare to a continuous signal that theoretically has an infinite number of data points.

As a result of our initial design, the initial electrical system was to consist of solar sensors, a voltage divider with a variable resistor, a comparator circuit, and an H-bridge. The solar sensors were to send separate electrical signals that would go through a voltage divider with a variable resistor. This would ensure that the sensors are calibrated to be "zeroed out" when getting equal light exposure. This signal is then sent to the comparator circuit that determines which sensor is getting more light exposure.

The H-bridge would then control the motor rotation (either clockwise or counter clockwise) until the sensors indicated equal light exposure.

In implementing our design, it became apparent that we needed to determine what options we had for each design block. And in addition, which of those options were optimal and would ultimately provide a working solar tracker. To improve the system's performance, design options were to be determined. This included what to use as solar sensors: solar cells, photodiodes, or photoresistors. Another very important consideration was to find what solar sensor arrangement was best. Meaning, what angle of separation between the two solar sensors would prove to give us the best sensitivity to a change in angle from the sun.

After actually implementation of our initial design, the analog comparator circuit was replaced with a digital microcontroller. This decision was made due to the fact that a microcontroller can provide more reliable results and improves the efficiency of the electrical system.

Analog Comparator & Motor Control

The main function of the solar sensors is to provide accurate and reliable tracking of the sun. Based on research of different ways to detect light, photoresistors, photodiodes, and photovoltaic cells were all deemed suitable for possible sensors. The benefit of these choices as solar sensors, and most sensor applications, is the fact that a sensor can provide a linear output with respect to the changing quantity that it is sensing. This allows for our design to remain as simple as possible. Specifically in our application, these sensors will output a voltage that has a linear relationship to the change in the angle of incidence. Another very crucial aspect to be considered about the solar sensors is we needed to choose a tilt angle between the sensors that would obtained the highest angular response.

In order to get accurate results for our solar sensor tests, we constructed an apparatus in which our solar sensors could be tested on. This started out as a piece of cardboard connected with a right angle. This gave us a structure to mount our sensors on. The only drawback to this was that we could not adjust the angle between the sensors: they could only be place at 45 degrees (a 90 degree angle between them). We acknowledged that this would not be suitable for further testing, so we were forced to create a new testing platform. We constructed a new apparatus that was made out of two blocks of wood connected with a hinge. This would allow us to vary the angle between the sensors from 0 to 180 degrees.

Solar Sensors

The main function of the solar sensors is to provide accurate and reliable tracking of the sun. Based on research of different ways to detect light, photoresistors, photodiodes, and photovoltaic cells were all deemed suitable for possible sensors. The benefit of these choices as solar sensors, and most sensor applications, is the fact that a sensor can provide a linear output with respect to the changing quantity that it is sensing. This allows for the design to remain as simple as possible. Specifically in this application, these sensors will output a voltage that has a linear relationship to the change in the angle of incidence. Another very crucial aspect to be considered about the solar sensors is the necessity to choose a tilt angle between the sensors that would obtained the highest angular response.

In order to get accurate results from the solar sensor tests, an apparatus was constructed in which the solar sensors could be tested on. This started out as two pieces of cardboard connected with a right angle. This allowed for a structure to mount the sensors on. The only drawback to this was that the angle between the sensors could not be adjusted: they were fixed in place at 45 degrees (a 90 degree angle between them). It was acknowledged that this would not be suitable for further testing, so a new testing platform needed to be constructed. The new apparatus was made out of two blocks of wood connected with a hinge in the middle. This would allow for varying of the angle between the sensors anywhere from 0 to 180 degrees. This apparatus can be seen in the figure below:

Figure 4 – Solar Sensor Testing Apparatus

Once the apparatus was set up, it was possible to test the light dependant resistors and

photodiodes by simply substituting them into the apparatus. The circuit that was utilized to test these

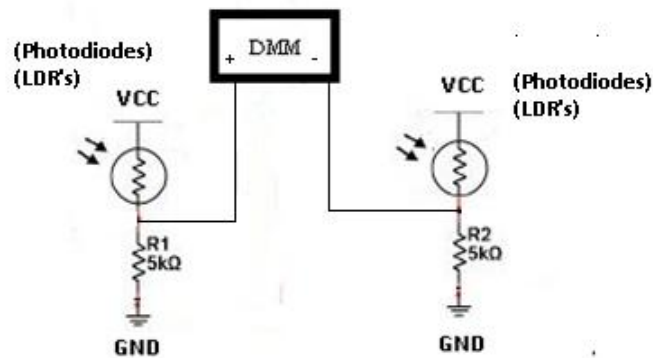sensors with the testing apparatus can be seen below:

Figure 5 – Solar Sensor Voltage Divider Circuit

LIGHT DEPENDANT RESISTORS:

As an initial attempt to get testing data from the solar sensors, light dependant resistors (LDR's) were tested in sunlight and with florescent room lighting. A LDR is a variable resistor that has a resistance linearly correlated to the amount of light it is exposed to. The starting point of the LDR's were at a perpendicular angle to the light source, then varying the angle over a span of 80 degrees. The light source that was used was a 80 watt light bulb, with a distance of 2 feet from the LDR's. The figure below represents the setup used to test the incidence angle of the light and tilt angles between the light sensors:
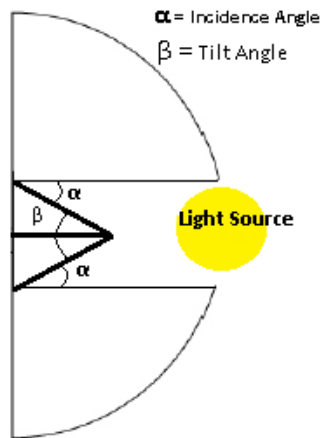
Figure 6 – Test Setup to Test Ideal Tilt Angle & Incidence Angle

The measurements seen in the figure below was made simply by measuring the resistance value across the LDR's with the use of a digital multimeter. The variance of 80 degrees for angle is due to the necessity of the solar tracker to have a vertical range of motion of 80 degrees. The results of this testing can be seen below:
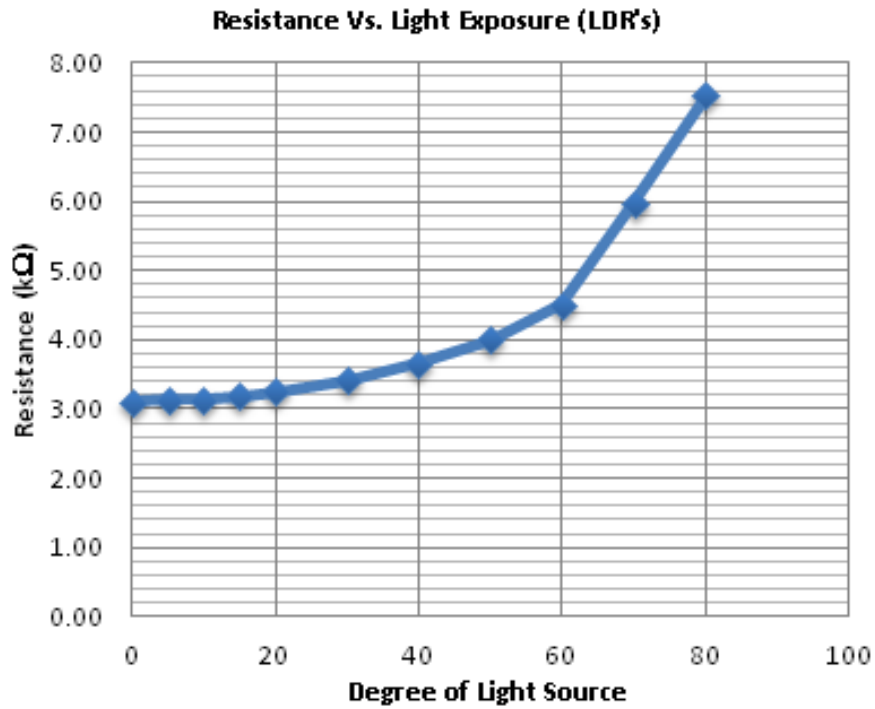
Figure 7 – Resistance of LDR's using 80 watt Light Bulb

The figure above displays the change in resistance of the LDR's while varying the angle of the LDR's with respect to the light source varying from 0 degrees (perpendicular) to 80 degrees (almost completely adjacent). This test was done with fluorescent lighting, which provided poor results due to the fact that the LDR's were not very sensitive to a small change in angle from the light source. It took a considerable change in angle to be able to get a moderate change in the resistance. The change in resistance only varied about 4.5K ohms.

Resistance Vs. Light Exposure (LDR's) (Sunlight)
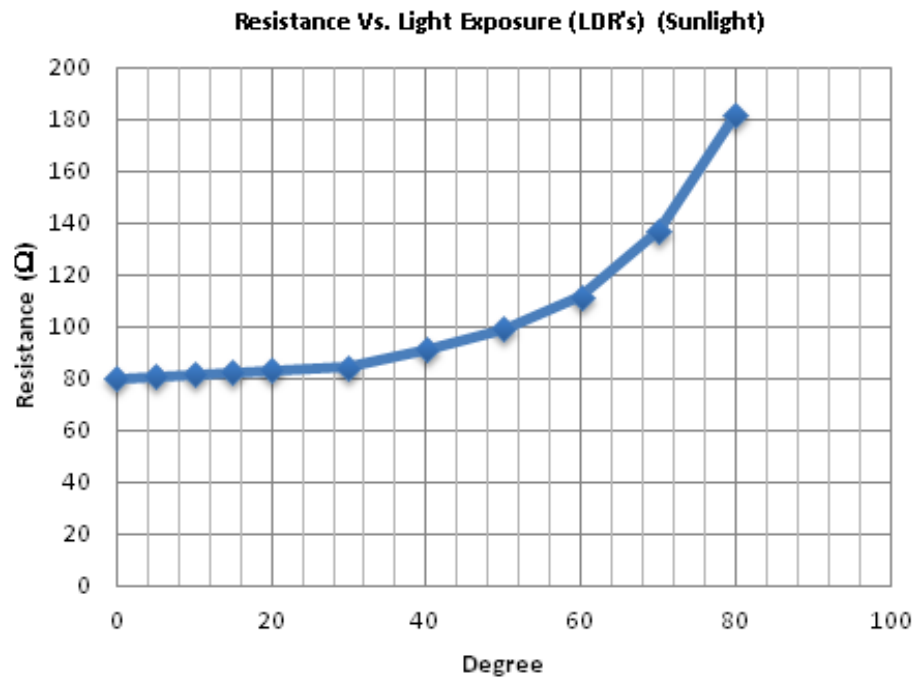
Figure 8 - Resistance of LDR's using Sunlight

The graph above displays the same test but with actual sunlight as the light source, instead of a fluorescent light bulb. This proved better results because the sunlight provided a better light source; the resistance of the LDR's was much lower than the resistance with the light bulb. Although, the change in resistance was much greater with the indoor application, this time resulting in a variance of only about 100k ohms. The major deficiency was again the fact that the LDR's were not very sensitive to a small degree change. Only with a large change in the incidence angle could a moderate change in resistance be realized.

Overall these setups with the LDR's provided poor accuracy for a small change in the incidence angle, which was the most important characteristic that the light sensors need to have. Despite these results, there was ultimately a need to test the angle between the two sensors to get an idea of how the voltage difference between the sensors would change by varying the tilt angle between the sensors. To test this, the solar cell apparatus was utilized. The incidence angle was varied from -90 to 90 degrees,

while the tilt angle between the cells was varied by 15 degree changes. The results can be seen in the
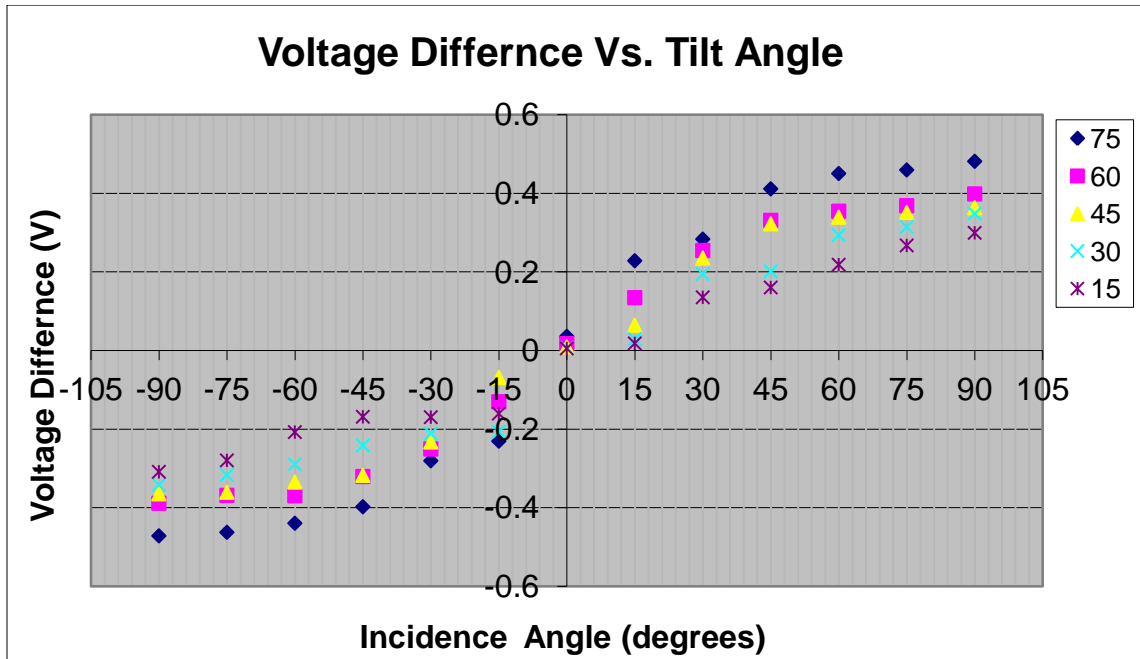
figure below:

Figure 9 – Tilt Angle Comparisons using LDR's

The testing of the LDR's tilt angle did prove to be useful even though the sensitivity of the

LDR's were not desirable. The test showed that the larger the tilt angle between the light sensors, the

more precision the sensors have. This information was usefully because it demonstrated that fact that a

large tilt angle between the solar sensors allows for a more accurate and reliable sensor array.

PHOTODIODES:

Another possibility for the solar sensors was the use of photodiodes. It was determined early that this would not be the best option because the photodiode do not provide the sensitivity that was required. It is capable of detecting a small incidence angle, but does not respond well when the sunlight when the photodiode is not perpendicularly facing the sun. Also the output voltage was so low that they would have needed considerable amplification to supply a sufficient voltage to the motor driver circuit and actuators. To test the photodiodes, they were substituted into the same circuit as was used for the LDR's. The same sensor apparatus and light source was utilized to test the angle between the photodiodes.
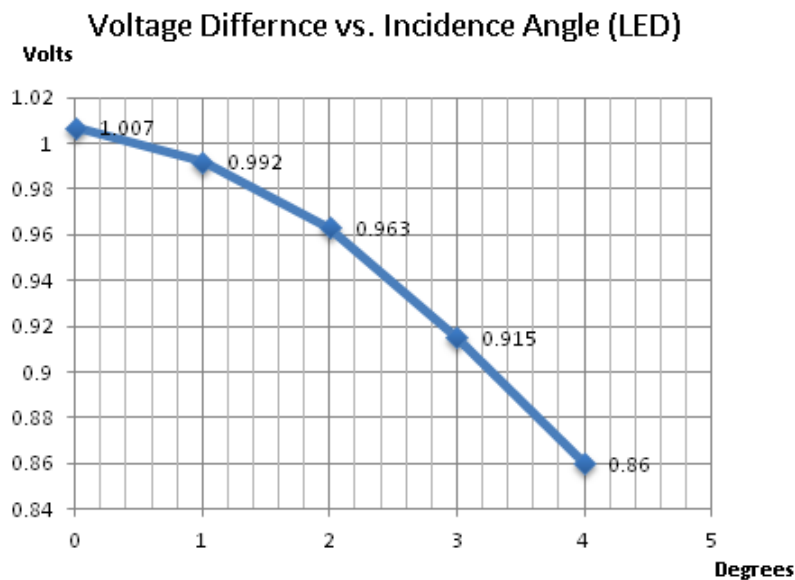

Figure 10 – Voltage Difference with Varying Incidence Angle (LED)

The figure above shows the use of a photodiode, comparing voltage difference (volts) and change in angle (degrees), being tested over a much smaller variance of the angle. This testing was done because ultimately it was required to get the sensor information while varying the incidence angle only a small amount. The sensitivity of the sensors will be determined from small variances in angles, not the large change of 180 degrees as was first tested. These results showed that use of the photodiode would

not be the best option. Even though it can detect a small change in the incidence angle, it does not produce a large enough voltage difference between the solar sensors. Ideally the solar sensors need to have the largest voltage difference as possible per degree change. This would constitute the greatest amount of sensitivity.

Using the 80 watt light bulb light source the LED produced a maximum of 1V, but the voltage outputs are inconsistent, so it is discarded as the choice of sensor for the solar tracker. However, in direct sunlight, the LED produced a voltage curve as shown in the figure below:
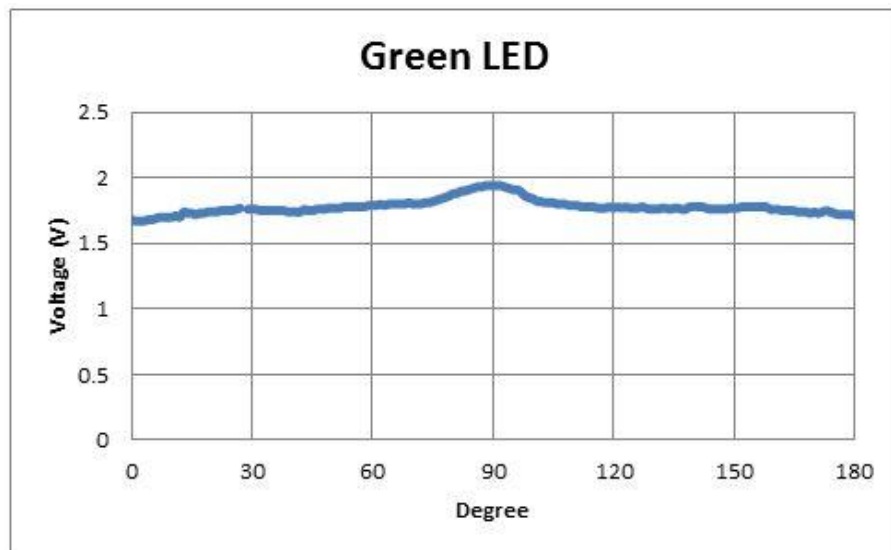
Figure 11 – Photodiode Output vs. Incidence Angle

The output voltage remains constant around 1.7V for degree from 0 to 60 and 120 to 180, but the voltage jump to 2V within a narrow region of 75 to 105 degree. It shows that LEDs are potential sensors for accurate light sensing in sunlight. That is why most home built solar tracker uses LED as the sensors. But this characteristic can only be seen when sensing sunlight, and not with the weak LED flashlight.

A major consideration with the solar sensor experiments was to find at what angle the two sensor pairs should be placed. This angle will determine the accuracy of the light sensor, and thus how well the tracker will actually function. The testing with the LDR's have already indicated that a higher angle

between the sensors will produce more sensitivity, but further testing was required. The data collected below was used to simulate how the sensor pairs would react depending on the angle of light incidence. The first figure displays the voltage difference between the LDR's, varying the tilt angle from 40 degrees to 80 degrees. The second figure shows the same information, only using the photodiodes.
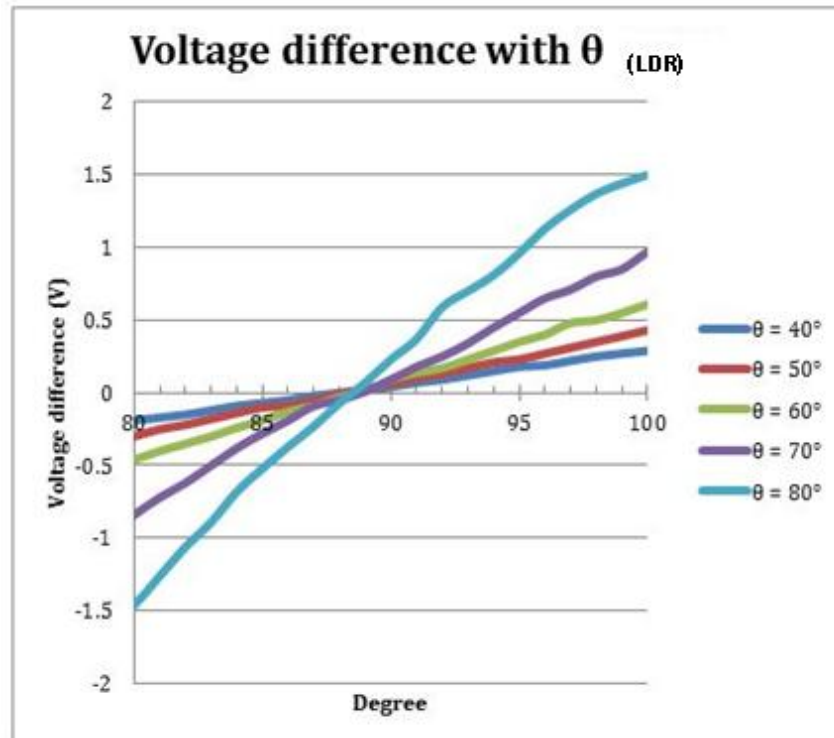

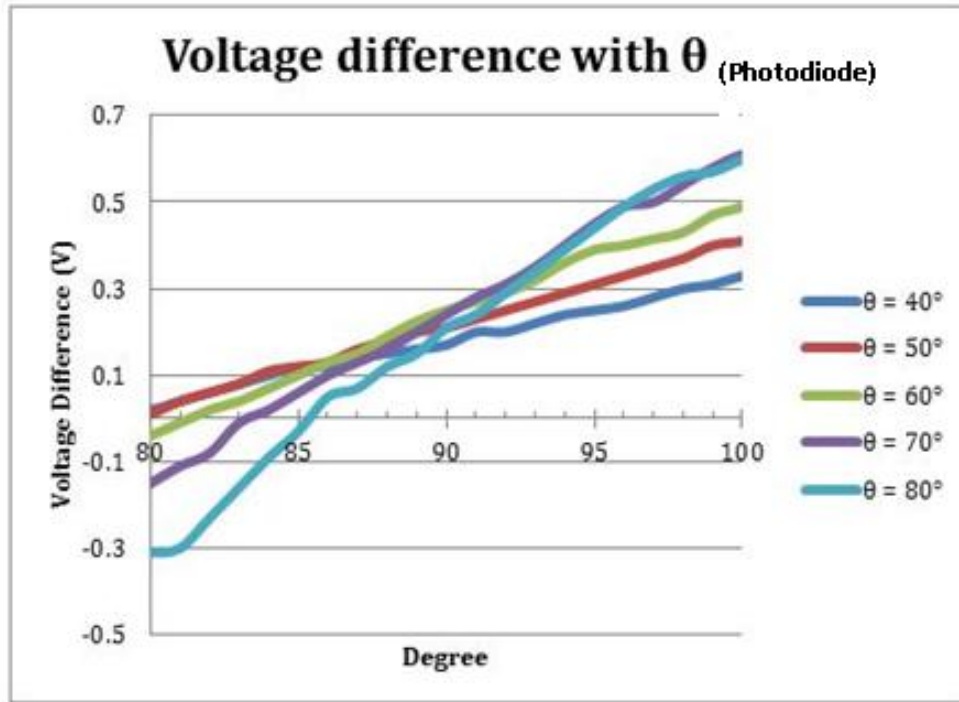**Figure 12 – Voltage Difference with different Tilt Angles (LDR's)**

Figure 13 - Voltage Difference with different Tilt Angles (Photodiodes)

From the data displayed above, the voltage difference is the highest when θ = 80 degrees for both LDR's and photodiodes. As predicted previously, the higher the voltage difference, the higher the sensitivity of the tracker. But the sensitivity for the LDR's were higher than the one for photodiodes. Thus choosing between LDR's and photodiodes, using the LDR's with θ = 80 degrees would produce the tracker with optimal sensitivity.

5.5.2. *Load Sensing Module*
<u>Load Sensor:</u>

<u>LOAD SENSOR:</u>

Apart from the designs for the solar sensor and driver circuits, another challenge to address was that of designing a load sensor to detect snow that may accumulate on the solar panel. The load sensor is designed to detect that a certain amount of weight has been placed on the solar panel. Once this weight

threshold has been crossed, the solar panel is to tilt to its 80 degree vertical maximum and holds there to allow the snow to slide off the panel. After the panel has been left tilted in a vertical orientation, it resumes its initial position and tracking continues. After researching, it was discovered that simple electrical principles and inexpensive materials could be utilized to make a functional load sensor.

It was determined that conductive foam (the same kind use to package IC's) has a linear relationship between compression and resistance. A piece of the foam has an initial resistance that represents no weight on it. But once a load is applied to the foam, the foam begins to compress, and the resistance across the foam starts to decrease.
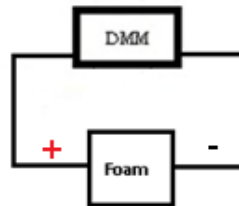

Figure 14 - Initial Foam Testing

To test this theory, a simple experiment was determined that involved passing two wires through a piece of the foam, as seen in the diagram above. The experiment entailed measuring the resistance values with a digital multimeter as increasing loads were applied. The foam that was used measured 2" x 1" x 1".
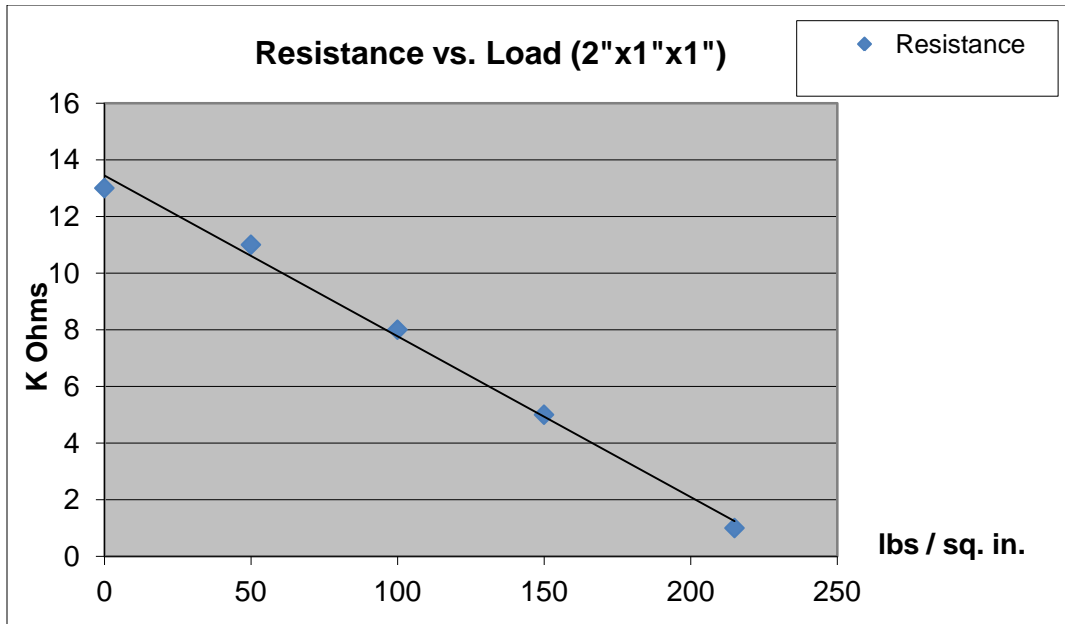
Figure 15 - Initial Foam resistance vs. load data

The data that collected is represented above and reinforced the theory that the foam would in fact decrease in resistance as weight was applied. However, that data itself and the way the experiment was conducted did not lead to satisfactory results. The technique of passing wires through the foam led to inaccurate results.

For the next iteration of this experiment, better documented specifications of the experiment and a better method for detecting the resistance across the foam was needed. To accomplish this, it was decided to place the foam between two metal plates and measure the resistance between the plates. This would provide more reliable resistance values than passing wires through the foam.

The foam that was to be used had already been chosen; next a determination as to what metal should be used as the conductive plates had to be made. The qualifications for the plates were a metal that provided good conductivity at the lowest cost.

Several highly conductive metals were considered including silver, copper, gold, aluminum, zinc, and brass. After narrowing down the list, keeping in mind conductivity and price, it was determined that copper or brass would make the best choices. Since pure copper is more expensive than brass, brass was chosen. Although brass's conductivity is only around 28% that of pure copper, it still provided an acceptable conductivity. Additionally, to ensure the conductivity of the brass, the plates used copper conductors and were brushed with steel wool to alleviate any electrochemical corrosion.

Next, two pieces of copper were cut to a size with enough surface area to be able to test by placing loads on it. The final cut of the plates were 5 7/8" x 4 ¾" each. The foam was then cut to the same size, with a thickness of .394". Testing of the resistance across the foam using the plates yielded much more accurate and usable results, seen below:
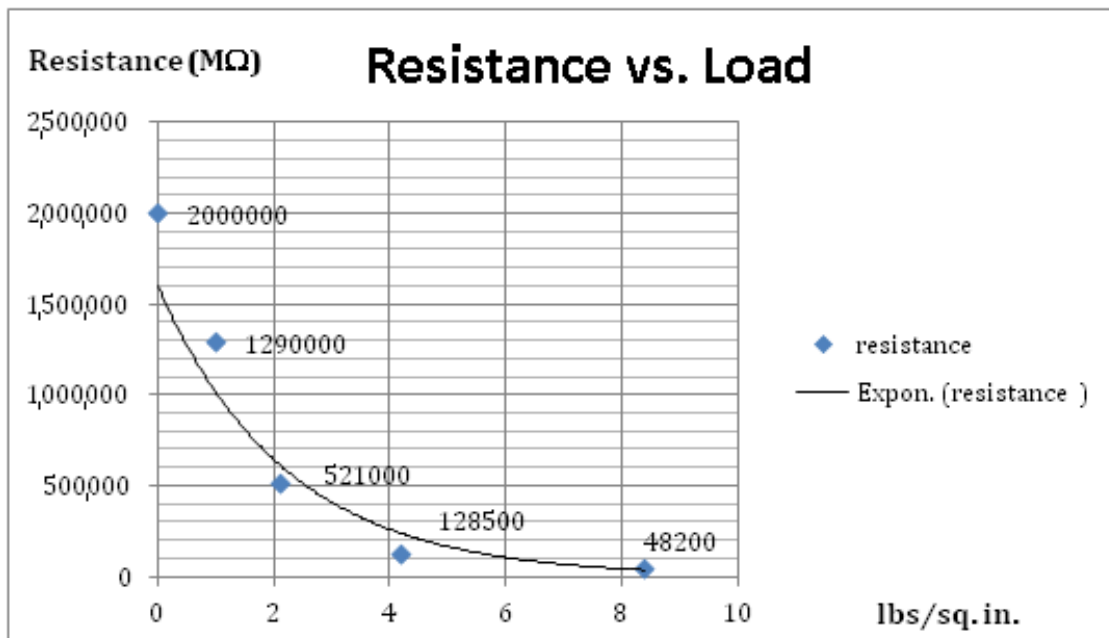

Figure 16 - Foam resistance vs. load w/ plates

These resistance values proved to yield acceptable results because by placing a load that did not correspond to a large amount of pressure, a large resistance drop was observed. Once the metals to be used for the plates had been chosen and tested for the sensor, the final step in the design was to determine a circuit that could deliver an analog signal for the microcontroller to process.

The simplest way to deliver an analog sensor signal to the micro controller was to use the load sensor in a voltage divider, considering the sensor itself as a variable resistor. A voltage divider is a set of two (or more) resistors connected in series between an applied voltage. The voltage at the points between the resistors is a fraction of the applied voltage, depending on the value of those resistances. This circuit was built so that it outputs a voltage, whose value increases with a decrease in resistance, or an increase in the load. A diagram of the circuit can be seen below:
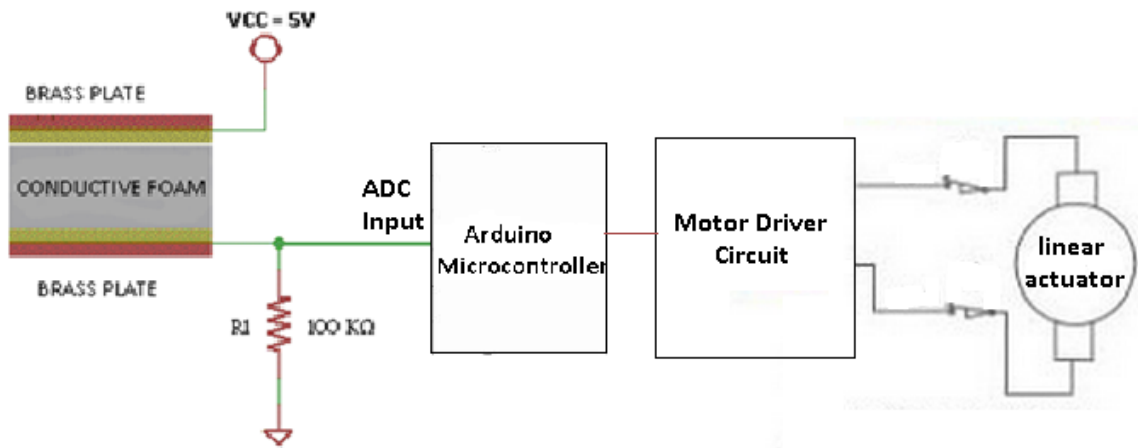

Figure 17 - Pressure Sensor Schematic

When a weight is placed on the load sensor, the resistance across the load sensor will decrease. This will cause the voltage drop across the load sensor to decrease as well.   This voltage drop is a

fraction of VCC, with the rest of the voltage being realized across R1. This voltage drop across R1 is the voltage seen at the microcontroller. This value starts as a small fraction of VCC when no weight is place on the sensor. But as weight increases, this voltage across R1 becomes equal and eventually surpasses the voltage across the sensor. The voltage across R1 is then sent to the 3rd analog input of the ADC of the Arduino microcontroller. The code for how the microcontroller processes this analog input is shown below:

```
float Pressure_Sensor = (analogRead(A3) * 5.0)/1023;//A3 is pressure sensor input


/*Whenever the load sensor input is higher than 2V, retract the linear actuator
until it is fully retracted

(the panel is at 80 degreees).

*/

if (Pressure_Sensor > 2.5) {

while(LA_Position > 0.2) {

digitalWrite(MotorCW, LOW);

digitalWrite(MotorCCW, HIGH);

}

}

if (diff > sensitivity) {

digitalWrite(MotorCW, LOW);

digitalWrite(MotorCCW, HIGH);

}

else if (diff < -sensitivity) {
```

```
digitalWrite(MotorCCW, LOW);

digitalWrite(MotorCW, HIGH);

}
```

When the arduino reads that the voltage across R1 is greater than 2.5V, and senses that the linear actuator is fully contracted for the 80 degree tilt, it orders the motor driver circuit that runs the linear actuator to turn the actuator motor counter clockwise. It will do this action until it senses that the linear actuator is fully contracted for its full 80 degree tilt. It will then hold there for 30 seconds, and then return to its initial position and continue tracking. If the arduino never senses that there is sufficient a load on the panel, it will just remain in its tracking mode.

To get even more accurate results from the sensor, further experimentation relating weight vs. resistance was conducted. This time, however, while the sensor was actually in the voltage diver circuit. These resistance readings were recorded using a digital multi-meter, as seen below:
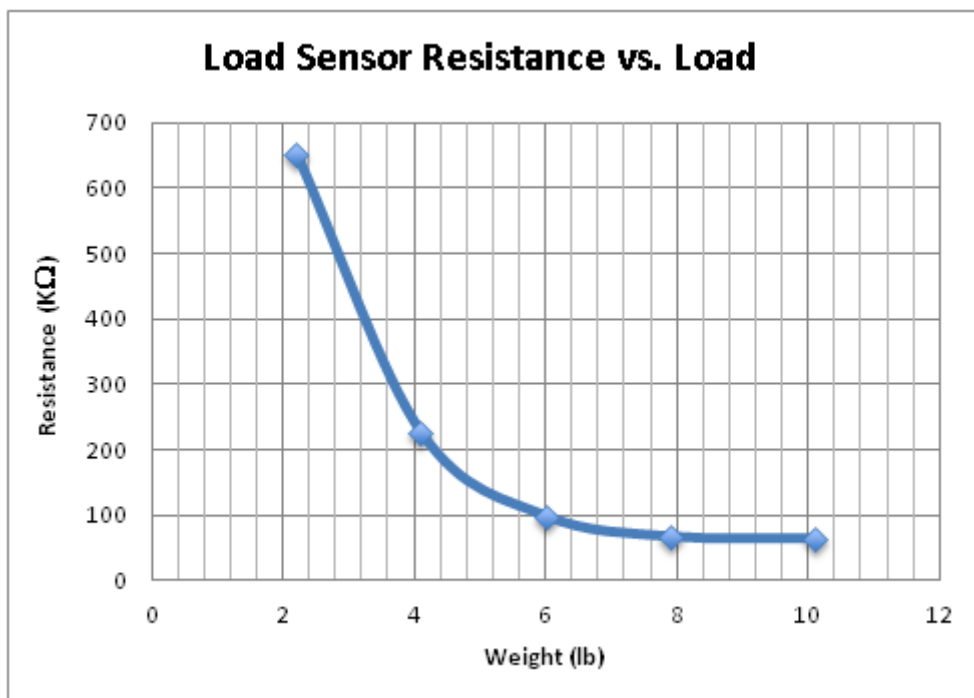

Figure 18 - Load Sensor Resistance vs. Load

The resistant readings were highly inaccurate with loads less than 2 lbs. However, the readings get more accurate with increasing loads. From simply looking at the figure above, a resistance between 200kΩ and 80kΩ should be place in series with the load sensor. The part of the graph that those loads correspond to gives the most accurate resistance readings.

After determining the value of R1 to be used, data was collected from the circuit in action. When a 5Vinput from the microcontroller is supplied to the circuit, the voltage across the 100kΩ resistor can be read by the microcontroller, which can order the solar panel to tilt whenever the voltage is more than 2.5V. This threshold is crossed at about 6lbs of pressure applied.
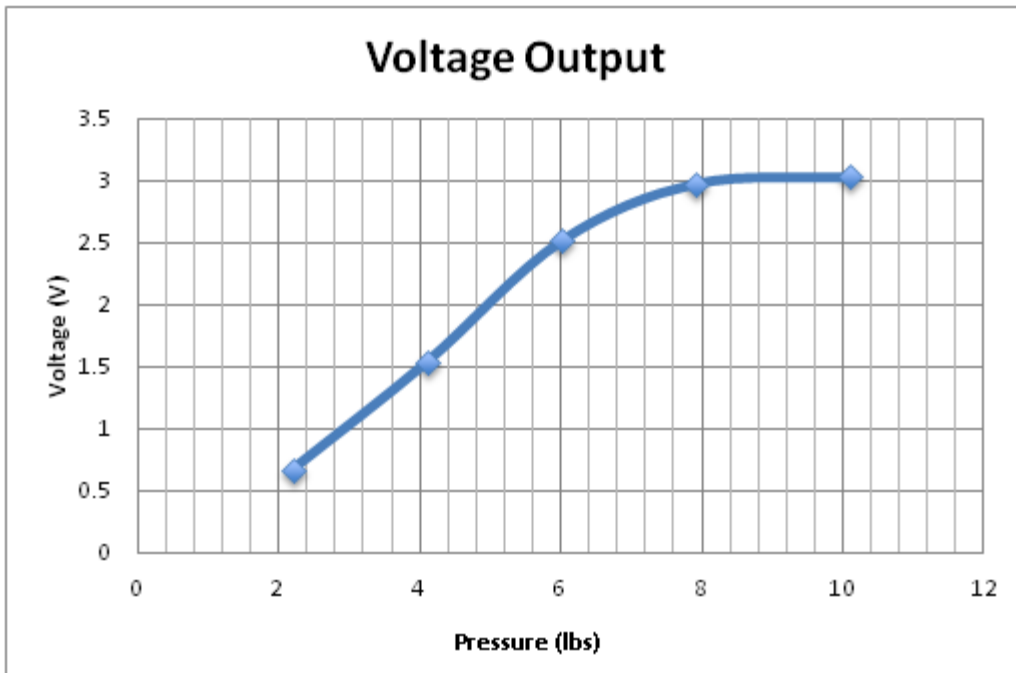

Figure 19 - Load Sensor Voltage vs. Load

From research it was determined that 1" of water corresponds to about 6 lbs per sq. ft. Considering that the water content of snow ranges from 5% to 45%, 1" of snow can vary from roughly 1/2 lb to 3 lbs. These values can even increase considering the fact that ice can accumulate as well. As can be seen from the figure below, that would correspond to about 10 inches of fluffy snow, and can be as little a few inches of very heavy snow. This threshold of 2.5V was chosen because it is important to eliminate a snow accumulation from the panel, even if the accumulation is relatively small in height. This is because the solar panel does not operate properly while having sections, or the entire panel, covered in snow. So once even a few inches has accumulated on the panel, it should be removed because it could inhibit the ability of the tracker to collect energy from the sun.
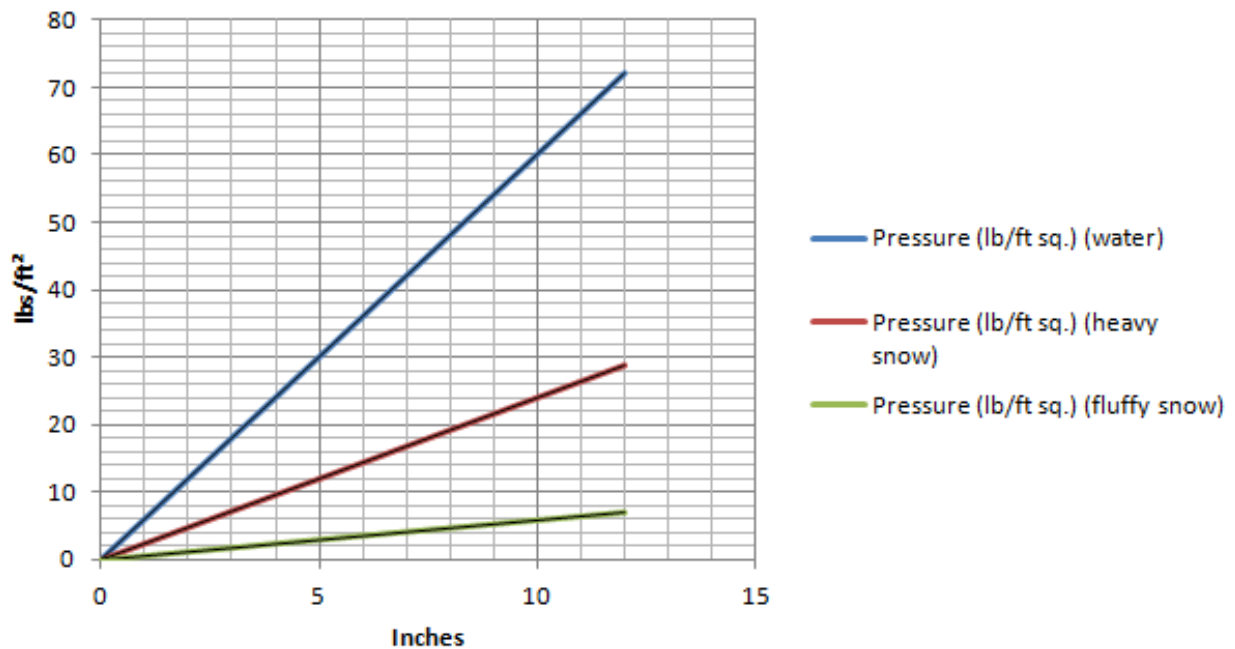

Figure 20 - Snow Weight vs. Thickness

POWER SUPPLY

The initial design for the solar tracker included a rechargeable battery using the energy collected from the solar panel to power the tracker. The battery would be continuously recharged by the solar pane, making the solar tracker would be totally self-sufficient. After consideration of the practical use of the solar tracker, it was decided that a rechargeable battery would not suit the application. The reasons for this being that the tracker would mostly be used indoors for demonstrational purpose. This would mean that the collection of light would be difficult, not able to sustain the tracker. Taking these things into consideration, it was determined that the tracker should have the capability of plugging into a wall outlet. This meant that the 120V 60Hz sine wave coming from a standard wall outlet needed to stepped down and rectified to a certain DC supply voltage that allowed the tracker to operate. This voltage was initially chosen to be 6V so that the linear actuator did not overshoot when moving from one point to another, but later changed to 12V.

There were many types of power supply designs that have been utilized. Most are designed to convert high voltage AC electricity to suitable, useable low voltage DC electricity. Although many of the designs were very similar in approach, in general a power supply can by broken down into a series of blocks, each of which performs a particular function. The blocks can be put in different orders, but the chosen block diagram of the power supply for the solar tracker can be seen in the figure below:
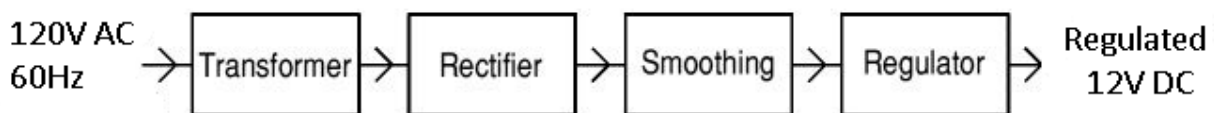

Figure 21 – Block Diagram for DC Power Supply

Each block of the figure above describes a different operation being applied to the 120V AC

voltage from the wall outlet to realize to a regulated 12V DC. The transformer is used to steps down

high voltage AC mains to low voltage AC. The transformer used had a 10:1 turns ration, meaning the

voltage is stepped down to 10% of that from the wall outlet: 12V AC. Next, the rectifier converts the AC

voltage to a DC, but the DC output at this stage is varying. This means that it is not a smooth DC voltage

but has a ripple voltage. The next block of the diagram is for smoothing. This part of the circuit will

smooth the DC voltage from varying greatly to a small ripple. This is generally accomplished by a

capacitor. Finally, the regulator block eliminates the ripple by setting DC output to a fixed voltage.

Additional components that were deemed necessary for the DC rectifier were: a switch to be able to turn

the supply on and off, a light to indicate that the supply is switch on, and a fuse to keep the transformer

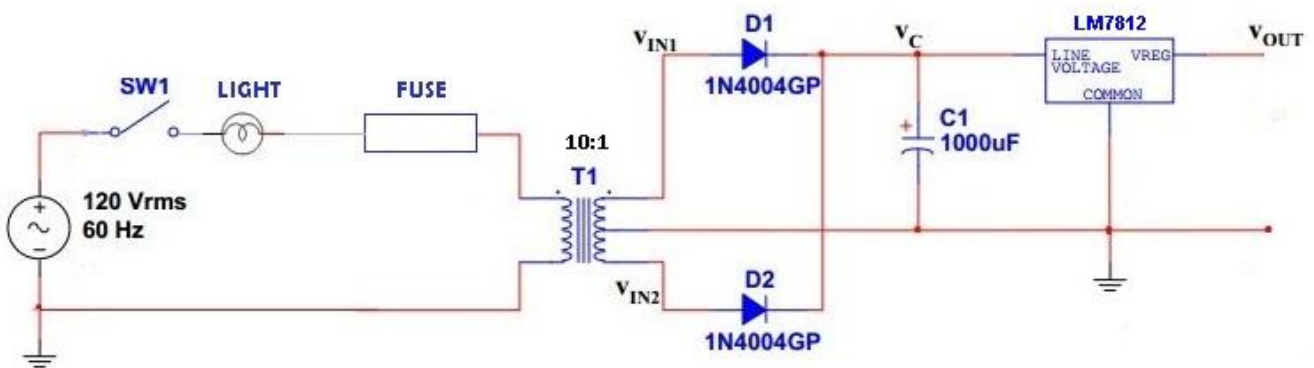and the tracker itself from being damaged.

Figure 22 – Regulated DC Power Supply

The figure above shows the actual implemented circuit that was used for the DC Power Supply.

It includes all of the components and stages previously described. A switch with a light was

implemented to indicate when the power source is on, along with a fuse to protect the tracker from voltage or current spikes as well as a short circuit.

The transformer is the first part of the circuit where DC rectifying takes place. Transformers convert AC electricity from one voltage to another with little loss of power. Step-up transformers increase voltage, step-down transformers reduce voltage. Most power supplies use a step-down transformer to reduce the dangerously high mains voltage (120V) to a safer low voltage. The input coil is called the primary and the output coil is called the secondary. There is no electrical connection between the two coils; instead they are linked by an alternating magnetic field created in the core of the transformer. Transformers waste very little power so the power out is almost exactly equal to the power in. It should also be noted that as voltage is stepped down, current is stepped up. This requires larger gauge wires from the output of the transformer to handle this current. The ratio of the number of turns on each coil, turns ratio, determines the ratio of the voltages. The step-down transformer, such as one used in the DC power supply, has a large number of turns on its primary coil which is connected to the high voltage mains supply, and a small number of turns on its secondary (output) coil to give a low output voltage. The transformer used for this DC power supply had a 10:1 turns ratio. The equation that governs the turns ratio can be seen below:

$$\text{Turns Ratio} = \frac{V_p}{V_s} = \frac{N_p}{N_s}$$

Figure 3 – Turns Ratio Equation

The figure above describes how the turns ratio for the transformer is calculated. V_p is the primary coil voltage, V_s is the secondary coil voltage, N_p is the number of turns on the primary coil, and N_s is the number of terms on the secondary coil. Thus, having a 10:1 turns ratio transformer means that the transformer is turning the 120V AC to 12V AC, and has 10 times as many turns on the primary coil than on the secondary coil.

The next part of the DC power supply is the rectifying stage. There are several ways of connecting diodes to make a rectifier to convert AC to DC. The bridge rectifier is the most popular and it produces full-wave, varying DC voltage. However, a full-wave rectifier can also be made from just two diodes if a center-tap transformer is used. Considering that the transformer used in the last stage is a center-tap transformer, it was possible to simply use 2 diodes, instead of the bridge rectifier which requires 4 diodes. Two diodes are still needed to create a full wave rectified signal. If only one diode is used, it would produce a half-wave rectifier output. Meaning, a single diode can be used as a rectifier, but this produces half-wave varying DC which leaves gaps when the AC voltage is negative. This makes it very difficult to smooth this sufficiently to supply electronic circuits with a DC voltage. This effect can be seen in the figure below:
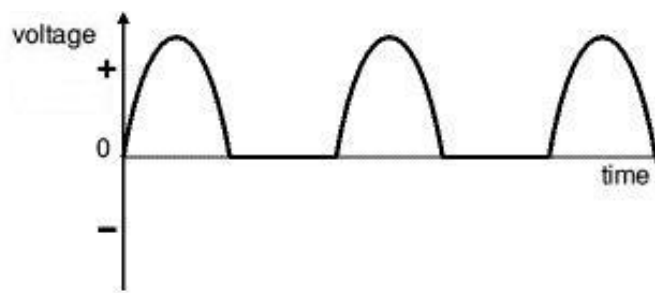
Figure 23 – Half Wave Rectified Signal

The problem of only have a half-wave voltage can be solved by simply using two diodes which creates a full wave voltage. This is accomplished by have one diode be active during the positive cycle of the AC signal, and the other be active during the negative cycle. This results in a waveform as seen in the figure below:
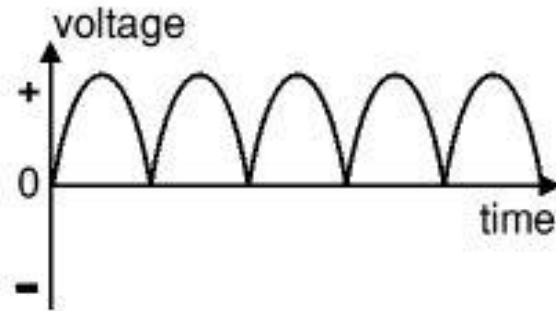
Figure 24 – Full Wave Rectified Signal

Once a full wave rectified voltage is achieved, there must be some sort of smoothing done to the waveform because a large ripple voltage still exists. This smoothing is performed by a large value dielectric capacitor connected across the DC supply to act as a reservoir, supplying current to the output when the varying DC voltage from the rectifier is falling. After using a 100uF capacitor to start, it was determined that a much large capacitance was required. The final circuit utilizes a 1000uF capacitor. The figure below shows the unsmoothed varying DC (dotted line) and the smoothed DC (solid line). The capacitor charges quickly near the peak of the varying DC, and then discharges as it supplies current to the output.
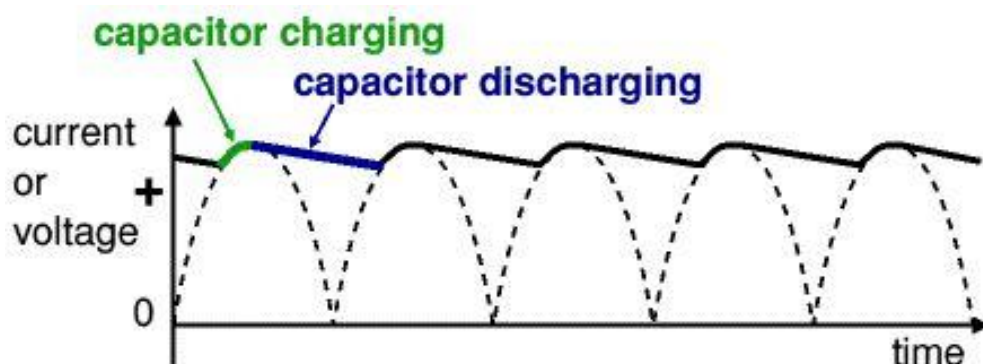
Figure 25 – Waveform Smoothing Utilizing a Large Capacitance

Although smoothing reduces the ripple voltage and helps create a DC waveform, it is not perfect. This is due to the capacitor voltage falling slightly as it discharges, giving a small ripple voltage. For many circuits a ripple which is 10% of the supply voltage is satisfactory, but a larger capacitor will give less of a ripple.

Once the ripple voltage has been made much smaller, the last piece of the circuit needed to complete the DC rectified waveform, thus creating the DC power supply, is voltage regulator. Voltage regulator ICs are available with fixed (typically 5V, 12V and 15V). In practice, DC power supplies utilize a voltage regulator IC whose job it is to maintain a constant output voltage to within tens of millivolts of the specified value. The voltage regulator chosen for this application was 12V because the DC power was determined to need to supply 12V to the DC motors. As can be seen from the figure below, the circuit configuration used was able to produce a clean 12V DC value. This power supply was deemed suitable to power the solar tracker.
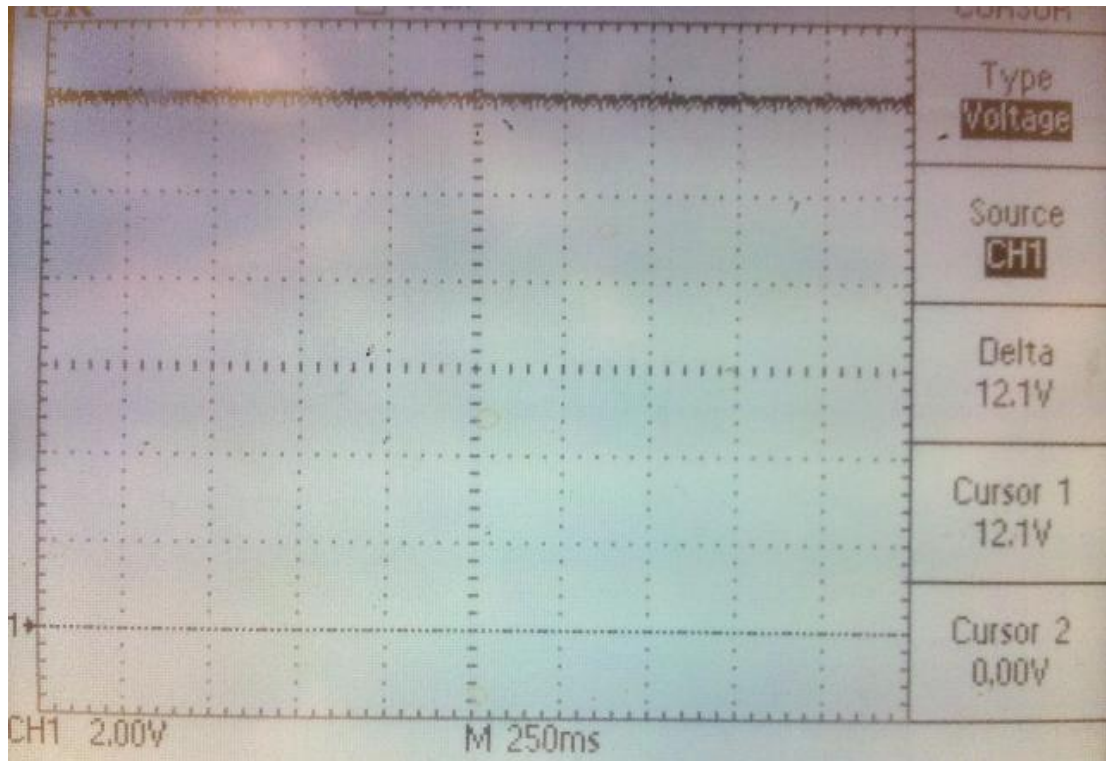
Figure 26 – Oscilloscope Image of 12V DC Output from the Power Supply

5.6. Stress, Strain and deflection

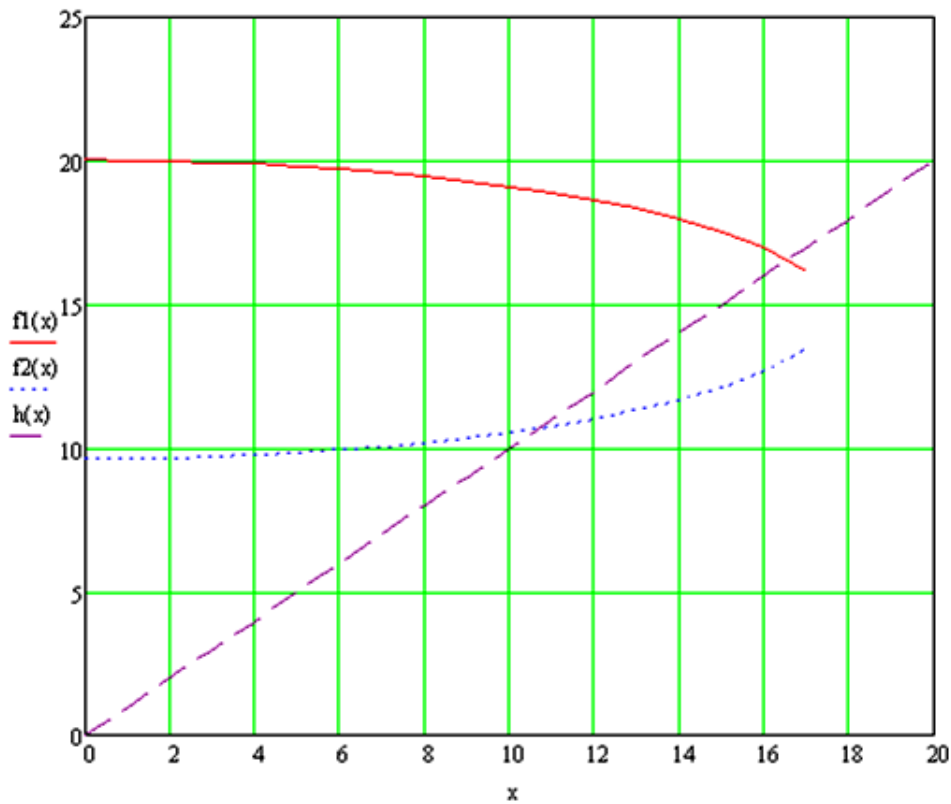## 5.7. Manufacturing

5.8. Assembly

Appendix A

$$a := 11.69 \qquad b := 17.59 \qquad x := 0,1..20$$

$$f1(x) := \frac{b^2 - a^2 - 2\cdot\sqrt{\left(b^2 - x^2\right)\left(4.59\cdot\sin(10)\right) + 4.59^2\cdot(\cos(10) - 1)^2 + (4.59\cdot\sin(10))^2}}{-2\cdot4.59\cdot(\cos(10) - 1)}$$

$$f2(x) := \frac{b^2 - a^2 + 2\cdot\sqrt{\left(b^2 - x^2\right)\left(4.59\cdot\sin(10)\right) + 4.59^2\cdot(\cos(10) - 1)^2 + (4.59\cdot\sin(10))^2}}{-2\cdot4.59\cdot(\cos(10) - 1)}$$

$$h(x) := x$$

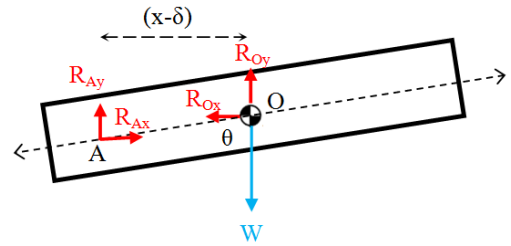$$f1(16.57) = 16.569 \qquad f2(10.69) = 10.69$$

Appendix B
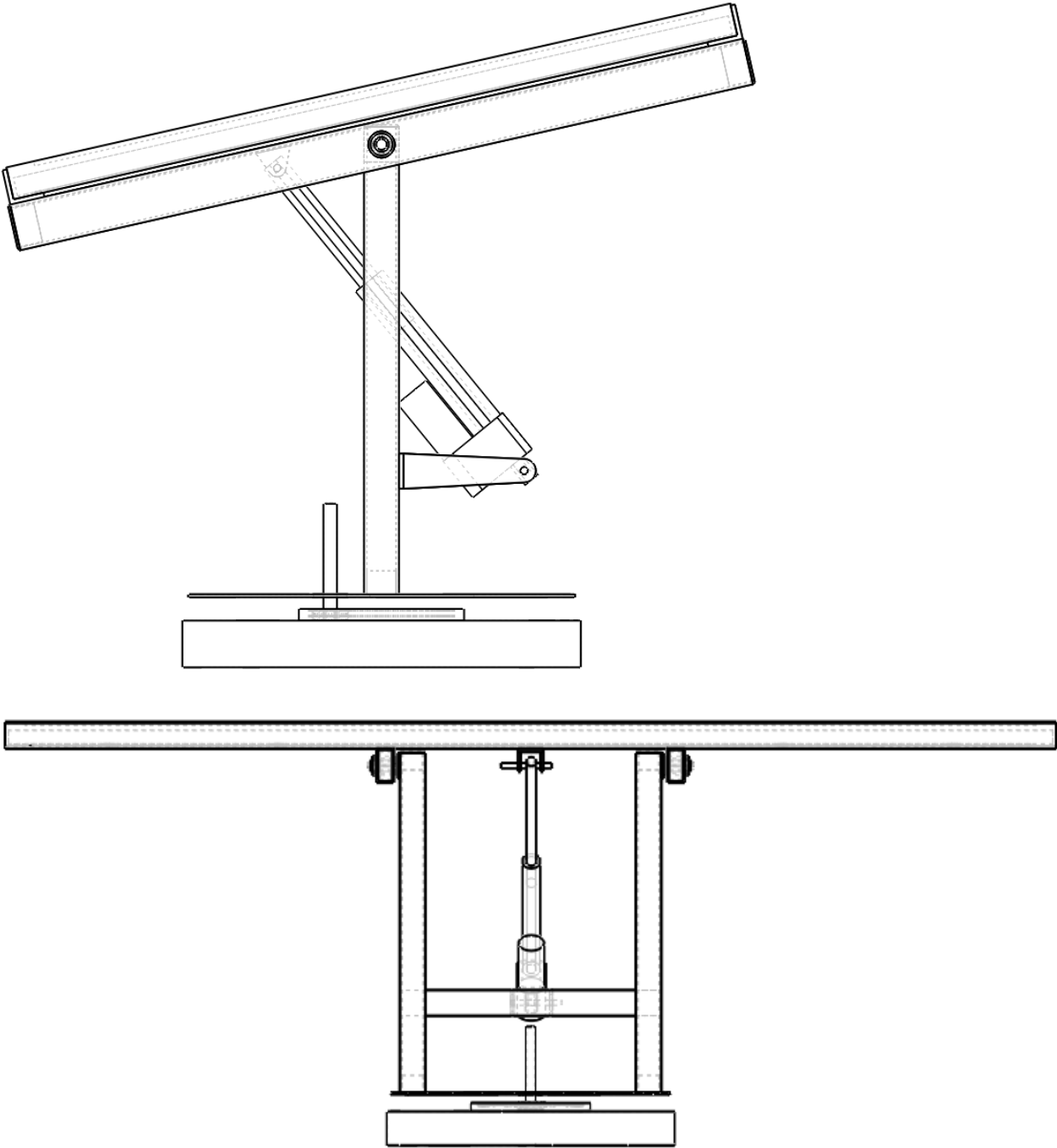
FBD of PV collector:

$$\sum F_x = R_{Ax} - R_{Ox} = 0 \qquad \Rightarrow \qquad R_{Ox} = R_{Ax}$$

$$\sum F_y = R_{Ay} - R_{Oy} - W = 0 \qquad \Rightarrow \qquad R_{Oy}$$
$$= W - R_{Ay}$$

$$\circlearrowleft \sum M_O = R_{Ay}(x - \delta)\sin\theta - R_{Ax}(x - \delta)\cos\theta = 0$$

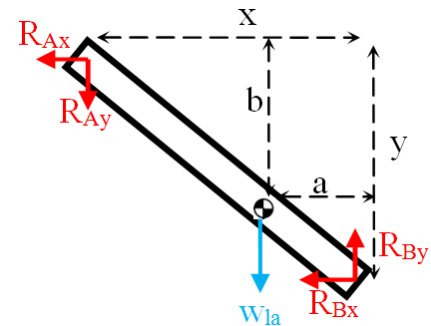$$\Rightarrow \qquad \frac{R_{Ax}}{R_{Ay}} = \tan\theta$$

FBD of linear actuator:

$$\sum F_x = R_{Ax} + R_{Bx} = 0 \qquad \Rightarrow \qquad R_{Ax} = -R_{Bx}$$

$$\sum F_y = R_{Ay} - R_{By} + w_{la} = 0 \qquad \Rightarrow \qquad R_{Ay} = R_{By} - w_{la}$$

$$\circlearrowleft \sum M_A = (x - a)w_{la} + yR_{Bx} - xR_{By} = 0$$

$$\Rightarrow \quad R_{By} = \frac{(x-a)w_{la} + yR_{Bx}}{x} \quad \Rightarrow \quad R_{By} = \frac{(x-a)w_{la} + yw_{la}\tan\theta}{x + y\tan\theta}$$
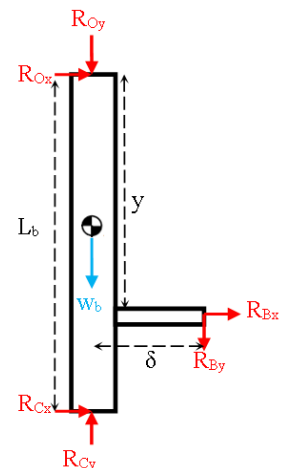
FBD of one vertical beam support:

All reaction forces that are in contact with other objects are halved since there are two vertical beams. Figure…shows forces on an equivalent single beam so that all forces obtained at contact places O and C will be halved on each beam

$$\sum F_x = R_{Ox} + R_{Cx} + R_{Bx} = 0 \qquad \Rightarrow \qquad R_{Cx} = -R_{Ox} - R_{Bx}$$

$$\sum F_y = R_{Oy} + R_{By} + w_b - R_{Cy} = 0 \qquad \Rightarrow \qquad R_{Cy} = R_{Oy} + R_{By} + w_b$$

$$\circlearrowleft \sum M_O = -L_b R_{Cx} - yR_{Bx} + \delta R_{By} = 0 \quad \Rightarrow \quad R_{Cx} = \frac{\delta R_{By} - yR_{Bx}}{L_b}$$

FBD of turn-table plate:

Assumptions:

1. All forces acting collinearly in a single plane

2. Cross section thickness chosen is so small that the slight curvature at the ends are almost straight lines when angle is small ($\tan \beta \simeq \beta$)

Considering cross section of circular turn-table in the y-z plane, since system is static, the force that motor shaft is exerting on the turn table is zero and therefore is not included in the plane of analysis. The turn table will be more prone to bending depending on the variables z_b and D. Distance z_b will in turn affect stability of the functional model and the angular momentum for dynamic motion.
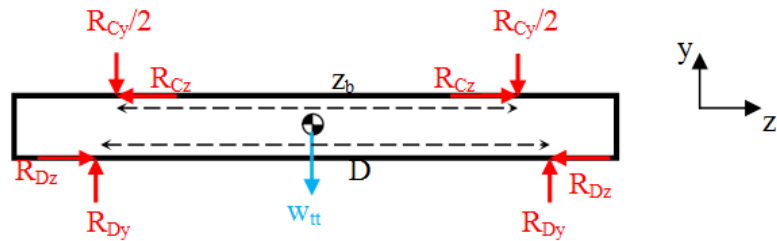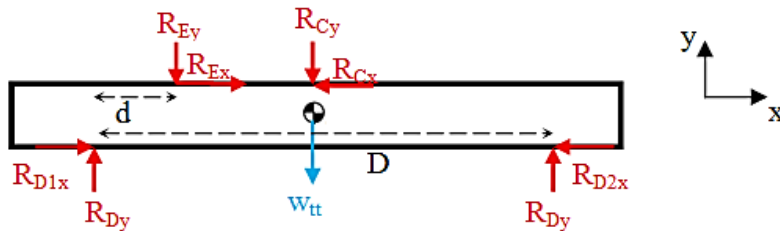

$$\sum F_z = R_{Cz} - R_{Cz} + R_{Dz} - R_{Dz} = 0$$

$$\sum F_y = R_{Cy} - 2R_{Dy} + w_{tt} = 0 \qquad \Longrightarrow \qquad R_{Dy} = \frac{R_{Cy} + w_{tt}}{2}$$

$$\circlearrowleft \sum M_C = \frac{z_b}{2} w_{tt} + \frac{z_b}{2} R_{Cy} + \frac{(D - z_b)}{2} R_{Dy} - (z_b + \frac{D - z_b}{2}) R_{Dy} = 0 \qquad \Longrightarrow \qquad R_{Dy} = \frac{R_{Cy} + w_{tt}}{2}$$

$$\circlearrowleft \sum M_{CG} = 0$$

$$\sum F_x = R_{Ex} - R_{Cx} + R_{D1x} - R_{D2x} = 0 \qquad \Longrightarrow \qquad R_{Ex}$$
$$= R_{Cx} - R_{D1x} + R_{D2x}$$

$$\sum F_y = R_{Cy} - 2R_{Dy} + w_{tt} + R_{Ey} = 0 \qquad \Longrightarrow \qquad R_{Ey} = 2R_{Dy} - w_{tt} - R_{Cy}$$
$$= 0$$

$$\circlearrowleft \sum M_{D1} = dR_{Ey} + \frac{D}{2} w_{tt} + \frac{D}{2} R_{Cy} - DR_{Dy} + tR_{Ex} - tR_{Cx} = 0 \Longrightarrow \qquad R_{D1x} = R_{D2x} = R_{Dx}$$

$$\Longrightarrow \qquad R_{Ex} = R_{Cx}$$

FBD of pinion and motor:

The gear set used is that of an internal gear set and the difference between external and internal gear set is that the former reverses direction of rotation between the cylinders whereas the latter will have the same direction of rotation on input and output shafts.

$$\sum F_x = R_{Fx} - R_{Ex} = 0 \qquad \Longrightarrow \qquad R_{Fx} = R_{Ex}$$

$$\sum F_y = R_{Fy} + R_{Ey} - w_p = 0 \qquad \Longrightarrow \qquad R_{Fy} = w_p - R_{Ey}$$

$$\Longrightarrow \qquad R_{Fy} = w_p$$
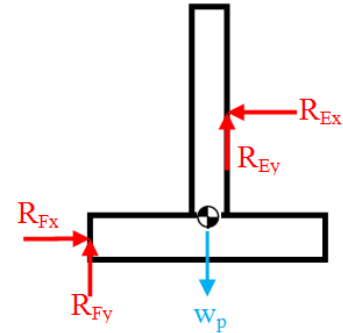
FBD of base and ball bearing:
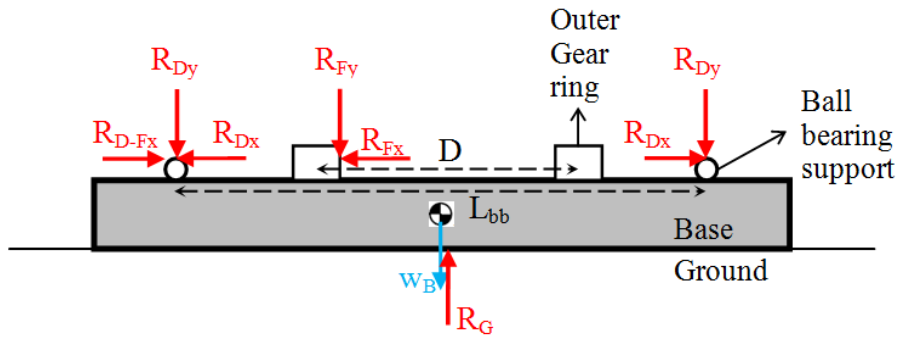
$$\sum F_x = R_{Dx} - R_{Dx} - R_{Fx} = 0$$

$$\sum F_y = 2R_{Dy} + w_B - R_G + R_{Fy} = 0 \qquad \Longrightarrow \qquad R_G = 2R_{Dy} + w_B + R_{Fy}$$

$$\Longrightarrow \qquad R_G = W + w_{tt} + w_{la} + w_p + w_b + w_B$$

Assumptions for static analysis:

2. Mass center of linear actuator is approximated to about 1/3 way from the more bulky end.

3. All connections are assumed to be point contact disregarding force distribution on objects in large surface contacts such as bolts and screws

4. All bodies are assumed to be rigid bodies

5. Materials have been approximately assigned to the bodies as either aluminum or steel to estimate the weights

6. CG of linear actuator is assumed to be the same whether extended or retracted based on the assumption that the pushing rod has negligible weight compared to the bulk part of the linear actuator itself